Cantilever-like micromechanical sensors

2011 Rep. Prog. Phys. 74 036101

(http://iopscience.iop.org/0034-4885/74/3/036101)

IOP PUBLISHING REPORTS ON PROGRESS IN PHYSICS

Rep. Prog. Phys. **74** (2011) 036101 (30pp) doi:10.1088/0034-4885/74/3/036101

Cantilever-like micromechanical sensors

Anja Boisen, Søren Dohn, Stephan Sylvest Keller, Silvan Schmid and Maria Tenje

DTU Nanotech–Department of Micro- and Nanotechnology, Technical University of Denmark, Bldg. 345 East, DK-2800 Kgs. Lyngby, Denmark

E-mail: anja.boisen@nanotech.dtu.dk

Received 25 May 2010, in final form 16 November 2010
Published 28 February 2011
Online at stacks.iop.org/RoPP/74/036101

Abstract

The field of cantilever-based sensing emerged in the mid-1990s and is today a well-known technology for label-free sensing which holds promise as a technique for cheap, portable, sensitive and highly parallel analysis systems. The research in sensor realization as well as sensor applications has increased significantly over the past 10 years. In this review we will present the basic modes of operation in cantilever-like micromechanical sensors and discuss optical and electrical means for signal transduction. The fundamental processes for realizing miniaturized cantilevers are described with focus on silicon- and polymer-based technologies. Examples of recent sensor applications are given covering such diverse fields as drug discovery, food diagnostics, material characterizations and explosives detection.

(Some figures in this article are in colour only in the electronic version)

This article was invited by H-G Rubahn.

Contents

1. Introduction

The field of cantilever-based sensing is still relatively young and was initiated in the mid-1990s. The research area has since then been rapidly increasing in terms of both number of publications and research groups involved. Micrometre-sized cantilevers hold promises as label-free, sensitive, portable, cheap, highly parallel and fast sensors for field use and have thus attracted considerable interest from applications such as point of care (POC) diagnostics, homeland security and environmental monitoring. Moreover, the sensors offer the possibility of measuring quantities and phenomena that are very difficult to achieve by other methods and they are therefore also very interesting fundamental research tools. Finally, the sensors can be operated in different modes which yield different information and which when combined can be used to obtain a unique set of coupled data. The sensors are versatile and can measure phenomena such as changes in surface stress, temperature and mass.

The sensing technique has already been featured and compared with other label-free sensor technologies in several review papers [1–7]. The focus of this review will be on

the instrumentation and recent fundamental scientific and technological advances. The review focuses on the cantilever geometry but will include a few related beam-based sensors with the same sensing principles.

Micrometre-sized cantilevers became available with the invention of the atomic force microscope (AFM) in 1986 [8]. Basically, the AFM functions as a miniaturized phonograph where images are obtained by raster scanning the surface with an AFM probe. The probe consists of a sharp tip mounted on a cantilever, which deflects due to the forces between tip and sample. The AFM probe needs to have micrometre dimensions in order to achieve a relative high resonant frequency (in the KHz regime) and a low spring constant (in the $\mathrm{N\,m^{-1}}$ regime). Typically, the cantilevers are 100 μm long, 50 μm wide and 0.5 μm thick. The high resonant frequency makes the probe less sensitive to external vibrations and the low spring constant improves the force sensitivity of the probe. Because of the small dimensions microfabrication is necessary. The first micromachined cantilevers with integrated tips were realized in 1990 by Tom Albrecht and co-workers at Stanford University [9] and by the group of Wolter at IBM [10].

Possibly inspired by some of the often encountered annoyances in AFM work Thomas Thundat and co-workers at Oakridge National Laboratory (Tennessee, USA) started in 1994 to explore the cantilevers' possible potential as a physical and chemical sensor [11]. Their initial work demonstrated that an AFM probe which is coated on one side with a metal layer for improved reflection of the laser beam will be prone to bimorph effects. This can cause severe drift problems in the AFM set-up. However, the effect can also be used as a simple principle for a very sensitive thermometer, where a static cantilever deflection can be related to a given temperature change. Moreover, it was demonstrated that a metal-coated cantilever kept at constant temperature responds reproducibly with a constant bending to humidity changes [11] and to exposure of other vapours such as mercury [12]. Also, it was showed that the amount of adsorbates can be estimated by monitoring shifts in the resonant frequency of the cantilever. Simultaneously, European groups started similar activities. The group around Mark Welland in Cambridge and the group around Jim Gimzewski and Christoph Gerber at IBM, Zürich, both used the bimorph effect to perform sensitive photothermal spectroscopy [13, 14]. Roberto Raiteri and Hans-Jürgen Butt from the Max-Planck-institute for Biophysics in Frankfurt reported on studies of surface stress changes induced electrochemically [15]. Unspecific binding of proteins to a hydrophobic surface was reported in 1996 [16]. The cantilever sensors can be used for online measurements of surface stress changes. This was demonstrated on a gold-coated cantilever exposed to alkanethiols [17]. These measurements illustrated that it is possible to follow the formation of a self-assembled monolayer (SAM) in real time, and the surface stress change was in this work seen to be related to the length of the alkane chain.

Most of the early cantilever-based sensing work was performed in standard AFM set-ups using normal AFM probes. In a normal AFM set-up it is only possible to measure on one cantilever at a time. This makes it impossible to simultaneously perform control measurements on a reference cantilever. The AFM probes used in the experiments typically had tips on, although for sensor applications this is not necessary. One of the first specifically designed large scale sensor systems was developed by Christoph Gerber and co-workers at IBM, Zürich. An array of polymer-coated silicon cantilevers was used to simultaneously detect the adsorption induced change in the surface stress of the cantilevers. The system could read-out from eight cantilevers simultaneously and different alcohols could be distinguished due to their different adsorption rates in the polymers [18]. Reference measurements on un-coated cantilevers were included here.

The potential of cantilever-based sensing in the field of diagnostics was highlighted in 2000 where it was demonstrated that a pair of cantilevers coated with two short strands of DNA-oligos that only differ by a single base can be used for single-nucleotide polymorphism detection [19]. These data were the source of many studies related to specific recognition of DNA, proteins and macromolecules.

On the technology side, cantilevers with integrated read-out started to appear in the late 1990s. The integrated read-out facilitates the realization of compact devices that can operate in even non-transparent environments. For example, in 2000 piezoresistive cantilevers for surface stress sensing were presented, demonstrating the possibility of realizing a dense array of sensors with a compact read-out system [20]. Even highly advanced systems with integrated electronics were soon demonstrated [21]. The field of self-sensing cantilevers has developed rapidly. Today several groups around the world are investigating different read-out techniques for the cantilever.

It is the aim of this review to give an overview of the expanding field of cantilever-based detection and to discuss fundamental issues regarding signal generation and interpretation based on recent experimental and theoretical findings. In section 2 we introduce the basic sensing principles, describing the generally used theoretical models and concepts of operation. The cleanroom-based fabrication techniques are introduced in section 3 with emphasis on new emerging materials such as polymers. The methods for reading out the cantilever deflection are described in section 4, which ends with a summary and comparison of the major read-out technologies used today. Recent examples on applications are described in section 5 and the review ends with general reflections on the future work on cantilever-based sensors in section 6.

2. Sensing principles

We will in the following concentrate on the use of cantilever-based sensors in the monitoring of changes in surface stress, bulk stress and mass depicted graphically in figure 1. In a first mode of operation, static deflection of the cantilever is measured. Change in static deflection is related to difference in surface stress of the two faces of the cantilever. This technique can be used to directly measure surface stress changes and as a sensing mechanism by functionalizing one surface of the cantilever with a specific detector layer (figure 1(*a*)). A bending will thus indicate whether material

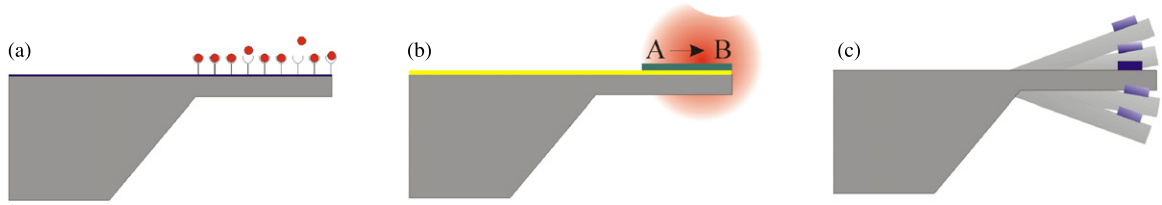

Figure 1. Schematic of three modes of operation of a cantilever-based sensor. The cantilever is seen from the side. Molecules on one side of the cantilever cause a change in surface stress which causes the cantilever to deflect (*a*). Bulk stress changes in the cantilever material can be used to detect temperature changes caused by a chemical reaction (*b*). Mass changes are registered by measuring changes in the resonant frequency of the cantilever (*c*).

has been interacting with the surface. If an added molecular layer, for example, contracts compared with the underlying material, the cantilever will bend towards the molecular layer. This measuring principle has been used to detect, for example, prostate-specific antigen (PSA) [22] and to study antibiotics binding to drug resistant super bugs [23]. A related technique to study surface stress changes is called the bending plate technique and was first observed and applied on wafers of III–V compounds in the 1960s [24]. By introducing the cantilever technique this measurement principle was significantly improved. Using the bending plate technique surface stress changes of $1\,\mathrm{N\,m^{-1}}$ were normally reported whereas the first measurements of surface stress changes with micrometre-sized cantilevers were of the order of $10^{-3}\,\mathrm{N\,m^{-1}}$. Now, surface stress changes of $10^{-6}\,\mathrm{N\,m^{-1}}$ are routinely observed.

In a second mode of operation the cantilever is used as a tool to evaluate stress changes in the bulk of the cantilever material, for example, caused by humidity or temperature. Stress changes are explored in the realization of extremely sensitive thermometers. Cantilevers consisting of two materials with different thermal expansion coefficients will bend as a function of temperature due to the bimorph effect. This effect can be used to measure temperature changes down to $10^{-5}\,\mathrm{K}$ and can, for example, be used to investigate phase changes in minute amounts of sample [25] (figure 1(*b*)).

In a third mode of operation the fact that the resonant frequency of the cantilever depends on the mass of the cantilever and the resonant frequency drops as the mass increases is used. Thus, it is possible to make indirect mass change estimations in the atto- to zepto-gram range [26] by following the resonant frequency change of the cantilever (figure 1(*c*)).

The change in static cantilever deflection or change in vibrational amplitude is most commonly detected by the so-called optical leverage technique which is well known from AFM. The principle will be described in section 4 and basically a laser is reflected off the backside of the cantilever and onto a position sensitive diode.

In nearly all experiments performed today a reference measurement is included. This means that a second cantilever with identical mechanical performance but without the specific surface funtionalization is monitored simultaneously. Often only the differential signals are presented since the use of reference measurements significantly reduces drift and noise from, for example, temperature and humidity changes.

2.1. Detection of mass changes

In mass sensing, cantilever and bridge shaped geometries are both commonly used and are in general referred to as beam-based mass sensors. Both geometries will be introduced in the following. A cantilever is a singly clamped beam whereas a bridge is a doubly clamped beam. One of the ultimate goals of a beam-based mass sensor is the ability to measure single small molecules which requires a sensitivity in the sub-zepto-gram (10^{-21} g) regime. This would, for example, make it possible to use a cantilever as a mass-spectrometer with sensitivity better than commercially available systems of today. The sensitivity or minimum detectable mass depends on the ratio between the mass and the resonant frequency of the beam. Generally, the resonant frequency increases and the mass decreases when the dimensions are decreased. Thus, a straightforward approach to enhance the sensitivity is to decrease the dimensions of the beam. The feature size of beam-based mass sensors is currently approaching the nanometre scale. Recently, systems capable of detecting masses in the atto- and zepto-gram (10^{-18}–10^{-21} g) range have been reported [27, 28], and the claim is that yocto-gram sensitivity is within reach [29]. This is far better than the reported mass sensitivities of other mass sensing techniques, such as the quartz crystal microbalance technique where typical sensitivities are in the nano/pico-gram range [30] for a single device. Sensors with a larger surface area generally have a relatively large distributed mass resolution (mass resolution per area). For example, so-called bulk disc resonators with micrometre dimensions now have similar distributed mass resolution as nanometre-sized cantilever resonators [31]. As a consequence, nanometre-sized resonators are useful when striving to achieve ultra-high point mass resolution. In terms of distributed mass resolution the benefit of miniaturization is less pronounced. Here, for example, micrometre [32] and nanometre-sized [33] cantilevers have been reported to have similar distributed mass sensitivities.

To explain the working principle of a beam-based mass sensor we will in the following introduce the equations describing the motion of a beam. Also, the importance of damping and Q-factor will be introduced.

2.1.1. The eigenfrequency of bending beams. For a thin beam as depicted in figure 2, rotational inertia and shear deformation can be neglected. Assuming a linear elastic material and small

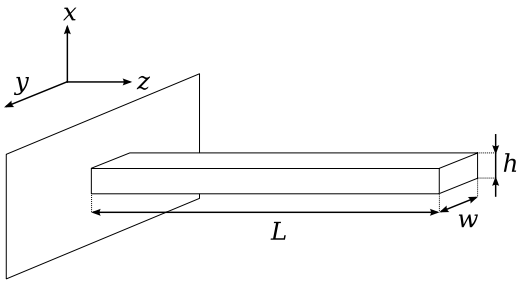

Figure 2. Schematic of a simple cantilever geometry.

deflections, the equation of motion is given by the Euler–Bernoulli beam equation [34]

$$\frac{\partial^2 U(z,t)}{\partial t^2}\rho\Gamma + \frac{\partial^4 U(z,t)}{\partial z^4}\widehat{E}I_z = 0, \tag{2.1}$$

where $U(z,t)$ is the displacement in the x-direction, ρ is the mass density, $\Gamma = wh$ is the cross-sectional area, $\widehat{E}$ is Young's modulus and I_z is the geometric moment of inertia. The solution to this differential equation is a harmonic that can be separated into a position dependent and a time-dependent term, $U(z,t) = U_n(z)\exp(-\mathrm{i}\omega_n t)$, where ω_n is the frequency of motion and where n denotes the modal number. By insertion into equation (2.1) the differential equation can be rewritten as

$$\frac{\partial^4 U(z,t)}{\partial z^4} = \kappa^4 U(z,t), \qquad \kappa^4 = \frac{\omega^2\rho\Gamma}{\widehat{E}I_z}. \tag{2.2}$$

The solutions (eigenfunctions) to the simplified beam equation (equation (2.2)) can be written in the form [35]

$$U_n(z) = A_n(\cos\kappa_n z - \cosh\kappa_n z) + B_n(\sin\kappa_n z - \sinh\kappa_n z). \tag{2.3}$$

The modal constants are determined from the boundary conditions. For a singly clamped beam (cantilever), the frequency equation becomes $1 + \cos(\kappa_n L)\cosh(\kappa_n L) = 0$ and the solutions for $n = 1, 2, 3, n > 3$ are $\lambda_n = \kappa_n L = 1.8751,\ 4.6941,\ 7.8548,\ (2n-1)\pi/2$, respectively. For a doubly clamped beam (bridge) the frequency equation is $1 - \cos(\kappa_n L)\cosh(\kappa_n L) = 0$ and the solutions for $n = 1, 2, 3, n > 3$ are $\lambda_n = \kappa_n L = 4.7300,\ 7.8532,\ 10.9956,\ (2n+1)\pi/2$, respectively.

The implication of the result is that a beam will vibrate in certain vibrational modes each with a distinct spatial shape. The first four such vibrational mode-shapes of a cantilever are shown in figure 3. It can be seen from the figure that certain areas of the cantilever have large vibrational amplitude whereas other areas (near the nodal points) are moving with low amplitude. The number of nodal points increases with increasing mode number.

The frequency of vibration of each of the mode-shapes is called the eigenfrequency and can be calculated from equation (2.2) and the corresponding solution of the eigenfunction (2.3). With the geometrical moment of inertia of a beam with rectangular cross section ($I_z = h^3 w/12$), the eigenfrequency of a bending beam is given by

$$\omega_n = \frac{\lambda_n^2}{L^2}\sqrt{\frac{\widehat{E}I_z}{\rho\Gamma}} = \frac{\lambda_n^2}{2\sqrt{3}}\frac{h}{L^2}\sqrt{\frac{\widehat{E}}{\rho}}. \tag{2.4}$$

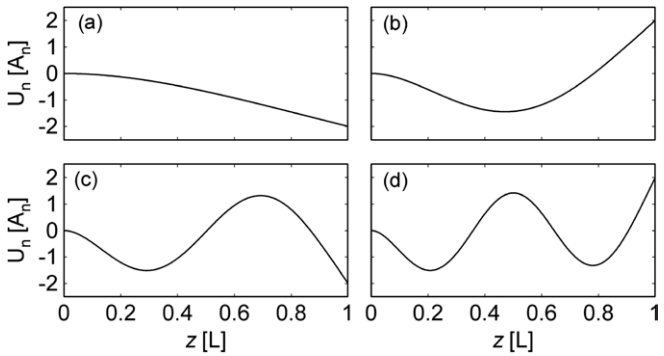

Figure 3. Schematics of the first four bending modes (*a*)–(*d*) of a cantilever seen from the side. The amplitude is in units of A_n and the position is in units of the length L, where 0 indicates the base of the cantilever.

If the beam width to height ratio $w/h > 5$, $\widehat{E}$ is replaced by $\widehat{E}/(1-\upsilon^2)$ where υ is the Poisson's ratio to account for the suppression of the in-plane dilatation accompanying axial strain [36].

Thin films typically used in microfabrication tend to have a process related tensile stress. Doubly clamped beams made of such thin films are therefore usually pre-stressed. A tensile stress σ increases the eigenfrequency and has to be taken into account by adding a term for the tensile force $N = \sigma\Gamma$ to (2.1). The free, undamped bending vibration for small amplitudes can then be described by

$$\frac{\partial^2 U(z,t)}{\partial t^2}\rho\Gamma + \frac{\partial^4 U(z,t)}{\partial z^4}\widehat{E}I_z - N\frac{\partial^2 U(z,t)}{\partial z^2} = 0. \tag{2.5}$$

This equation of motion can be solved for a simply supported doubly clamped beam with $\lambda_n = n\pi$. The eigenfrequency of a doubly clamped bending beam with an axial force is then given by [37]

$$\omega_n = \frac{(n\pi)^2}{L^2}\sqrt{\frac{\widehat{E}I_z}{\rho\Gamma}}\sqrt{1 + \frac{NL^2}{(n\pi)^2\widehat{E}I_z}}. \tag{2.6}$$

A beam with rectangular cross-section is approaching pure beam-like behaviour if $12\sigma L^2 \ll (n\pi)^2\widehat{E}h^2$ and (2.6) reduces to (2.4). On the other hand, if $12\sigma L^2 \gg (n\pi)^2\widehat{E}h^2$ the flexural rigidity can be neglected and (2.6) reduces to

$$\omega_n = (n\pi)\frac{1}{L}\sqrt{\frac{\sigma}{\rho}}, \tag{2.7}$$

which is the eigenfrequency of a string with a displacement function [38]

$$U_n(z) = C_n \sin\left(\frac{n\pi}{L}z\right). \tag{2.8}$$

It is commonly used to simplify the beam-dynamics of an individual resonance mode with that of a harmonic oscillator:

$$\omega_0 = \sqrt{\frac{k_{\mathrm{eff}}}{m_{\mathrm{eff}}}}, \tag{2.9}$$

where k_{eff} and m_{eff} denote effective spring constant and effective mass. For the first bending mode of a cantilever the specific spring constant and the effective mass are given by

$$m_{\mathrm{eff}} = 0.24 m_0, \quad m_0 = \rho\Gamma L, \qquad k_{\mathrm{eff}} = \frac{\widehat{E}h^3 w}{4L^3}. \tag{2.10}$$

2.1.2. Sensitivity and resolution. From equation (2.9) it is clear that the resonant frequency depends on the vibrating mass. The change in resonant frequency due to a change in mass is called the sensitivity S of a resonant mass sensor. This is a very important parameter for bending beam-based mass sensors, since it in turn will determine the minimum detectable mass.

Assuming that the change in mass, Δm, is very small compared with m_0 and distributed evenly over the entire resonant beam surface, the mass sensitivity of a beam can be found by differentiation of equation (2.9) with respect to the mass of the beam:

$$S = \frac{\partial \omega_0}{\partial m_{\text{eff}}} = -\frac{\omega_0}{2m_{\text{eff}}} \approx \frac{\Delta\omega_0}{\Delta m}, \tag{2.11}$$

where $\Delta\omega_0$ is the change in the resonant frequency caused by an added mass, Δm.

To obtain a high sensitivity a beam must have a high resonant frequency, which can be obtained by having a large Young's modulus, low density and small dimensions. Furthermore, it must have a low mass, requiring a low density and small dimensions. Thus, for bending beams a higher sensitivity can be obtained at higher vibrational modes due to a decreasing effective mass at higher modes [39]. Also, doubly clamped beams have higher resonant frequencies than singly clamped beams of same dimensions. However, the vibrational amplitude is smaller and the doubly clamped structures are therefore in general more difficult to read-out.

The resolution, that is the smallest detectable mass of the sensor, Δm_{min}, is given by the inverse sensitivity times the minimum detectable frequency change $\Delta\omega_{\text{min}}$:

$$\Delta m_{\text{min}} = S^{-1}\Delta\omega_{\text{min}}. \tag{2.12}$$

The frequency stability and thereby $\Delta\omega_{\text{min}}$ is determined by the noise of the system originating from both the read-out circuitry and the resonator itself [29].

2.1.3. Damping and noise. A beam with a kinetic energy will experience damping and thereby dissipation of its kinetic energy. The dissipation is defined as the ratio of energy lost per cycle to the stored energy, and is the inverse of the quality factor (Q-factor). The damping will cause a broadening of the resonant peak and introduce frequency noise, thereby increasing the minimum detectable change in frequency.

Dissipation occurs through several mechanisms that are either intrinsic to the cantilever or due to extrinsic processes. The intrinsic processes are, among others, material damping (phonon–phonon interactions, phonon–electron interactions, thermo-elastic damping) [40–42] and anchor losses [40, 43, 44]. Extrinsic dissipation occurs due to interactions with the surrounding media and can be controlled by mode of operation and atmospheric pressure. The total dissipation is the sum of all contributions

$$\frac{1}{Q} = \sum \frac{1}{Q_{\text{int}}} + \sum \frac{1}{Q_{\text{ext}}} = \frac{1}{Q_{\text{air}}} + \frac{1}{Q_{\text{mat}}} + \frac{1}{Q_{\text{anc}}} + \frac{1}{Q_{\text{sur}}} + \cdots.$$

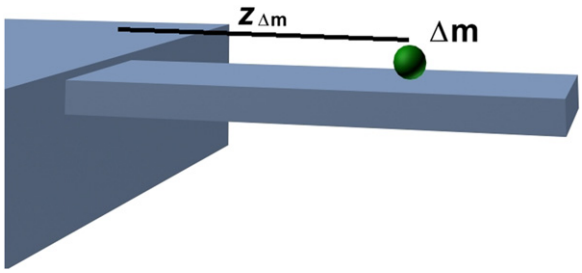

Figure 4. Schematic of a cantilever with a single bead, having the mass Δm, positioned at $z_{\Delta m}$.

For bending beam resonators operated under ambient conditions viscous damping or momentum exchange with the surrounding medium is the dominant source of dissipation, giving rise to low Q-factors (around 100) [29]. Thus, high-sensitivity beam-based mass sensors are generally operated at low pressures [45]. If a beam is a sandwiched structure, such as a metal-coated silicon cantilever, material damping can be dominant [46, 47].

Pre-stressed doubly clamped beams have been seen to have extraordinary high quality factors [48] and in polymeric doubly clamped beams the material damping is significantly reduced when the beams become string like [49]. Clamping loss is one of the limiting damping effects for resonant strings [49, 50]. By improving the clamping, quality factors of up to 4 million have been obtained with silicon nitride micro-strings [51].

Often, beam-based mass sensors are affected by noise attributed to individual molecules that adsorb and desorb on the surface of the beam [29]. This process changes the mass and thereby the resonant frequency of the beam. Also, the read-out system introduces noise which is associated with the transduction of the mechanical response into an electrical signal and which is highly dependent on the method of choice [27, 52–57].

2.1.4. Position dependent mass measurements. In the previous section the mass of adsorbed molecules is assumed to be distributed uniformly over the beam surface. This approach is not viable if single molecules or particles are to be measured, since the change in resonant frequency is not only dependent on the mass of the attached particle but also on the position on the beam [39, 58, 59]. This is due to the shape of the vibrational modes. The areas of the beam with a large vibrational amplitude are areas where an added mass will gain a high kinetic energy and thereby change the resonant frequency considerably compared with the nodal points where no energy is transferred from the beam to the added particles.

Consider a cantilever with the mass m_0 loaded with a point mass Δm positioned at $z_{\Delta m}$ (figure 4). If the mass load is much less than the cantilever mass, $\Delta m \ll m_0$, the cantilever mode-shape will not change significantly, and the resonant frequency of such a system can be accurately estimated using an energy approach. According to Rayleigh's method the time average kinetic energy, E_{kin}, equals the time average strain energy, E_{strain}, at resonance [60].

Assuming a small deflection and thereby neglecting shear stress, the energy of a deflected cantilever is the energy stored due to the induced strain. The eigenfrequency of a cantilever can be derived by equalizing the kinetic with the strain energy:

$$E_{\text{strain}} = E_{\text{kin}} + E_{\text{kin},\Delta m}. \tag{2.13}$$

The kinetic energy for the cantilever loaded with a mass, Δm, is

$$E_{\text{kin}} = \tfrac{1}{2} m_0 \omega_{n,\Delta m}^2, \tag{2.14}$$

where $\omega_{n,\Delta m}$ is the frequency of motion and n is the modal number. The kinetic energy of the added point mass at $z_{\Delta m}$ is

$$E_{\text{kin},\Delta m} = \tfrac{1}{2} \Delta m \omega_{n,\Delta m}^2 U_n^2(z_{\Delta m}). \tag{2.15}$$

Assuming that the mode-shape will not change significantly due to the added mass, the strain energy in the cantilever is approximately equal to the kinetic energy of the cantilever without the added mass:

$$E_{\text{strain}} \approx \tfrac{1}{2} m_0 \omega_n^2. \tag{2.16}$$

With (2.13), the eigenfrequency of the cantilever with the added mass becomes

$$\omega_{n,\Delta m}^2 = \omega_n^2 \left(1 + \frac{\Delta m}{m_0} U_n^2(z_{\Delta m})\right)^{-1}. \tag{2.17}$$

The position dependent mass responsivity can now be calculated for a given position, $z_{\Delta m}$, of the adsorbed mass Δm:

$$\begin{aligned} S_{\text{point}} &\approx \frac{\Delta \omega_n}{\Delta m} = \frac{\omega_{n,\Delta m} - \omega_n}{\Delta m}, \\ S_{\text{point}} &\approx \frac{\omega_n}{\Delta m}\left(\sqrt{1 + U_n(z_{\Delta m})\Delta m / m_0}^{-1} - 1\right). \end{aligned} \tag{2.18}$$

For $z_{\Delta m} = L$ the mass responsivity exhibits the same mode dependence as the mass responsivity of a uniform distributed mass, $S_{\text{point},L} \propto \lambda_n^2$. But, the mass responsivity is also highly dependent on the position and for $z_{\Delta m} \neq L$ the mass responsivity has a complicated dependence on the mode-number and must be calculated for each position and mode.

Knowing the mass responsivity and a measured change in resonant frequency it is possible to calculate the mass of the molecules or particles forming a homogeneous layer on the cantilever using equation (2.12). That is

$$\Delta m_{\text{meas}} = S^{-1} \Delta \omega_{\text{meas}}. \tag{2.19}$$

If a single point mass is adhering to the cantilever, and the change in resonant frequency of several modes are measured, both position and mass can be calculated. Using the approach of Dohn *et al* [59] the position can be found by minimizing

$$\chi^2 = \sum_{n=1}^{N} \left(\frac{\omega_{n,\Delta m}}{\omega_n} - \frac{1}{\sqrt{1 + (\Delta m / m_0) U_n^2(z_{\Delta m})}}\right)^2 \tag{2.20}$$

with respect to the position and where N is the total number of modes measured. The position minimizing equation (2.20) yields the most likely position of the adhering point mass. The mass can subsequently be calculated. The calculation of a point mass based on resonant frequency measurements can be extended to multiple point masses [61] and a similar approach to determine position and mass has been developed for strings [62].

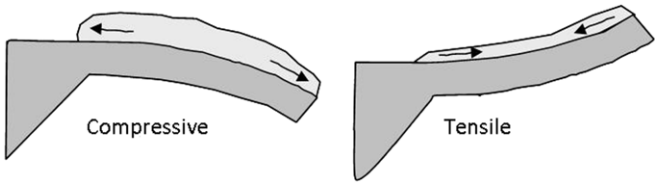

Figure 5. Stress in a thin film on a cantilever. The relative film thickness is highly exaggerated for clarity. As the film expands the cantilever bends down. The resulting stress in the film is compressive as its expansion is hindered and balanced by the bending of the cantilever. For a contracting film the cantilever bends up and the resulting stress in the film is tensile.

2.2. *Detection of surface stress changes*

Molecules that adsorb on a cantilever do not only add a mass but also generate a surface stress due to interactions between the molecules and the cantilever surface. In 1909, Stoney developed a theory to measure surface stress/elastic strain of a thin film deposited onto a sheet of metal [63]. Although Stoney studied thin metal films, this equation is still used to quantify the surface stresses generated in molecular/chemical thin films from different molecular recognition events. Stoney's formula is given by

$$R = \frac{\widehat{E} h^2}{6\sigma(1 - \upsilon)}, \tag{2.21}$$

where R is the radius of curvature, $\widehat{E}$ is Young's modulus, h is the thickness of the metal sheet, σ is the surface stress generated and υ is Poisson's ratio of the metal sheet. In 1966 Stoney's formula was further developed by Jaccodine and Schliegel [64] to be applicable to cantilever structures that are clamped at one side, which introduces some mechanical limitations compared with a free sheet of metal. Now the surface stress, σ, is related to the cantilever deflection, Δz, via the length of the cantilever, L:

$$\Delta z = \frac{3(1 - \upsilon) L^2}{\widehat{E} h^2} \sigma. \tag{2.22}$$

From here it is seen that the deflection can be optimized by decreasing the thickness and increasing the length of the cantilever.

Stoney's formula requires that one knows Young's modulus of the cantilever. In particular, in situations where more exotic materials are used for cantilever fabrication this might be a major source of error. The group of Grütter has re-worked Stoney's formula to overcome this issue [65]. Today, a modified Stoney's formula is available for cantilevers with only nanometre thickness [66] that might be realized in the near future. Stress changes in a thin film on the surface of a cantilever are illustrated in figure 5. In figure 5(*a*) the cantilever bends downwards and expands until the stress thus created in the cantilever balances the stress in the thin film on top. The stress in the film is compressive as the expansion is hindered by the supporting cantilever. The stress on the top side of the supporting cantilever is tensile. In the case of a contracting film the cantilever bends upwards and the stress in the thin film is said to be tensile (figure 5(*b*)).

2.2.1. Origin of surface stress—experimental focus. Although the equation for measuring the surface stress from a cantilever deflection has been available for more than 100 years, the origin of the surface stress and the relation to the force transduction (chemical recognition event to mechanical deflection of the cantilever) has been under dispute and is still not clarified within the research community. There exist a few theoretical papers that try to decipher the fundamental physics of the origin of surface stress [67–69]. These papers are not linked to experimental studies. In this section, we will focus on the most relevant experimental findings existing within the community. For clarity, we only consider studies of DNA hybridization and alkanethiol layers.

DNA hybridization is studied in two steps. First, single-stranded DNA (ss-DNA) is immobilized on a cantilever. The actual hybridization event takes place when a complementary ss-DNA strand is introduced, resulting in a hybridized double-stranded DNA (ds-DNA) bound to the cantilever. The first proposal on the physics of surface stress came in 2000 from Fritz *et al*, where it was suggested that the surface stress originates from electrostatic, steric and hydrophobic interactions [19] between the hybridized DNA strands on the cantilever. It was observed that the DNA hybridization event causes a compressive surface stress. DNA strands hold a net negative charge. It is argued that the electrostatic interaction changes since ds-DNA has a larger number of charges compared with ss-DNA. The steric contribution is believed to arise from a denser chain packing as a result of the hybridization. A year later, Wu *et al* [70] showed on-line measurements of a cantilever first being functionalized with ss-DNA and then exposed to complementary DNA for hybridization. The immobilization step resulted in a large compressive stress whereas the hybridization event resulted in a small tensile stress. Their findings indicated that the cantilever deflects in the opposite direction as to what Fritz *et al* reported. Furthermore, the cantilever was observed to bend in opposing directions for the ss-DNA immobilization and the subsequent ds-DNA hybridization. Intuitively this is rather surprising as one might simply expect the cantilever to bend more (in the same direction) as more molecules are added to the surface. To explain the experimental results, Wu *et al* argued that the surface stress cannot be a result of electrostatic and steric interactions alone. They proposed to also consider configurational entropy, which is related to the order of the immobilized molecules. The ss-DNA has a significantly lower persistence length than ds-DNA (under the same buffer conditions), which means that the ds-DNA has a higher stiffness and is more rod like. As a result, the cantilever is required to bend more to ensure sufficient space for the ss-DNA strands to form a SAM. The ds-DNA in turn will not force the cantilever to deflect as much since it requires less space to form a SAM due to its more rigid structure. Therefore, when Wu *et al* started with a blank cantilever and introduced ss-DNA for immobilization they observed a compressive stress on the cantilever. When the complementary strands were introduced to form the ds-DNA this stress was released (since a more ordered SAM could be formed). They then observed a tensile stress/release of compressive stress.

However, this does not explain why their findings contradict the findings of Fritz *et al* with respect to DNA hybridization. To further support their theory on the significance of the configurational entropy, Wu *et al* immobilized ss-DNA on two different cantilevers in a 1M buffer. These cantilevers were then exposed to two different hybridization conditions. In the first situation, DNA was hybridized under the same buffer conditions (1M) and a tensile stress was observed. In the second situation, the buffer concentration was reduced to 0.1M before the complementary ss-DNA strand was introduced. The change in buffer concentration forced the ss-DNA to form a more ordered monolayer. In turn, a compressive stress was observed during hybridization. This clearly indicates that configurational entropy plays a role in signal generation and it stresses the importance of controlling all aspects of a cantilever measurement (buffer conditions, pre-treatments, temperature variations, etc) since several effects are involved in generating the surface stress signal.

The group of Rachel McKendry has studied the origin of surface stress in a methodical manner. In 2002 [71] the influence of the physical steric crowding of molecules on a cantilever was pinpointed as the main contributor to the cantilever deflection for DNA hybridization. It was seen that the hybridization signal is close to non-existent when the density of probe ss-DNA is tailored for maximized hybridization efficiency. Again, this indicates that molecules with 'sufficient space' do not generate a cantilever deflection.

In 2007, the effects of electrostatics [72] were investigated. Here, simple SAMs of thiolated *n*-alkane chains with different end-groups were used as model system. The active SAM had carboxyl-groups at the end, which could be protonated/deprotonated upon pH variations. The main physical effect of the cantilever deflection in this situation was assigned to electrostatic repulsion and ionic hydrogen bond formation. Emphasis was also put on the counter ions present in the aqueous solution; these can affect both the magnitude and direction of the cantilever deflection. Figure 6 shows the contribution from each individual effect (electrostatic repulsion and ionic hydrogen bond formation) as well as the effective interactions. Experimental data are also plotted and seen to agree well with the proposed theory.

In 2008, McKendry, Sushko and co-authors proposed the 'first quantitative model to rationalize the physics of nanomechanical sensors' [73]. Here, a theoretical model is developed that predicts the cantilever deflection direction and magnitude upon pH variations of the buffer solution and for various chain lengths of SAMs. The model considers the effects of chemical, elastic and entropic properties of both cantilever material and sensing layer.

Recently, the group of Grütter [74] analysed the effects of intermolecular electrostatics, Lennard-Jones interactions and adsorption-induced changes in the electronic density of a metal film when thiolated alkane chains are immobilized on a gold-coated silicon cantilever. Their findings indicate that it is the latter effect combined with the associated electronic charge transfer from the gold to the thiol bond that account for the largest contribution to the measured surface stress. These

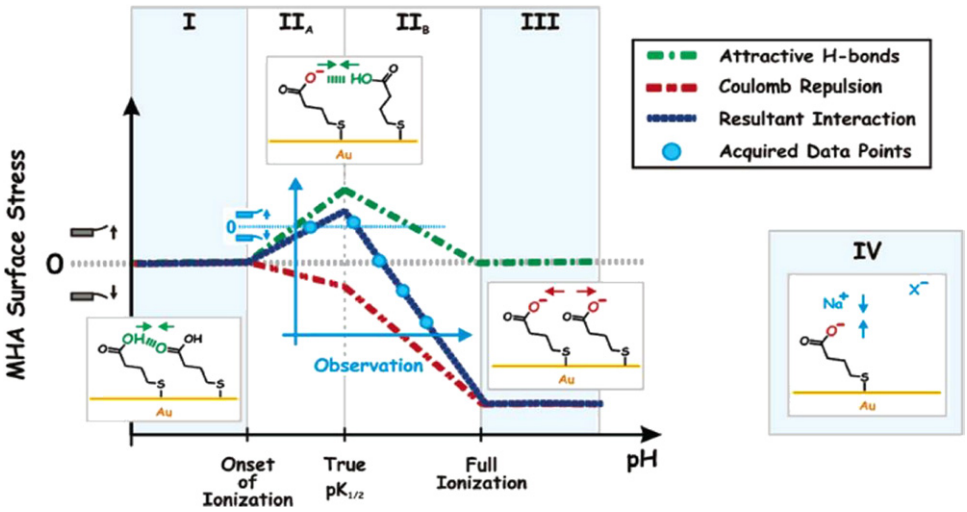

Figure 6. As the pH of the buffer solution is changed from 4.5 to 9.0 the cantilever displays both tensile and compressive stress as the carboxyl group at the end of the SAM goes from fully protonated (region I) to fully ionized (region III). The insets illustrate the proposed molecular configuration on the gold-coated cantilever surface at different pH values [72].

findings bring something completely new to the community and the manuscript even proposes a method to enhance the surface stress signal: one should enable anions from the measuring solution to come in contact with the metal surface, to give an increased cantilever deflection, see figure 7. This could possibly be obtained by either using a sensing layer with pinholes or by using a sensing layer that deforms and opens up after the molecular recognition event has occurred.

2.2.2. Effect of gold layer. Gold is a preferred cantilever coating in combination with thiol chemistry. In 2001 it was noted that the cleanliness of the gold surface is highly influential on the resulting surface stress signal generated from the self-assembly of thiolated alkanechains [75]. The generated surface stress after an injection of hexanethiol was observed for a gold layer (i) stored under ambient conditions for ten days and (ii) gold cleaned in either 33% aqua regia or (iii) 5 min O_2/N_2 plasma. From the measurements it could be seen that cleaning the gold surface significantly increases the cantilever deflection. A difference between the cleaning methods was also noted, with the aqua regia cleaning method generating the largest surface roughness and the largest surface stress signal.

Both Godin *et al* [76] and Mertens *et al* [77] have investigated the effect of the gold topography on the resulting cantilever deflection. Godin *et al* have compared gold coatings with (>500 nm) and (<100 nm) grains. Both gold layers have been functionalized with dodecanthiol and it is concluded that the resulting cantilever deflection is largest for the (>500 nm) grains. It is argued that highly uniform SAMs with all molecules in the 'standing up' phase can only be obtained when the SAM is not interrupted by grain boundaries. Mertens *et al* presented somewhat opposite findings. Here, the cantilever deflection was seen to be larger for gold coating with small (∼20 nm) grain sizes than for larger grains (∼100 nm). However, it should be noted that the studied grain sizes and immobilization procedures are different. Mertens *et al* argue that a large number of grain boundaries results in a large surface area which consequently increases the possibility for molecules to adsorb.

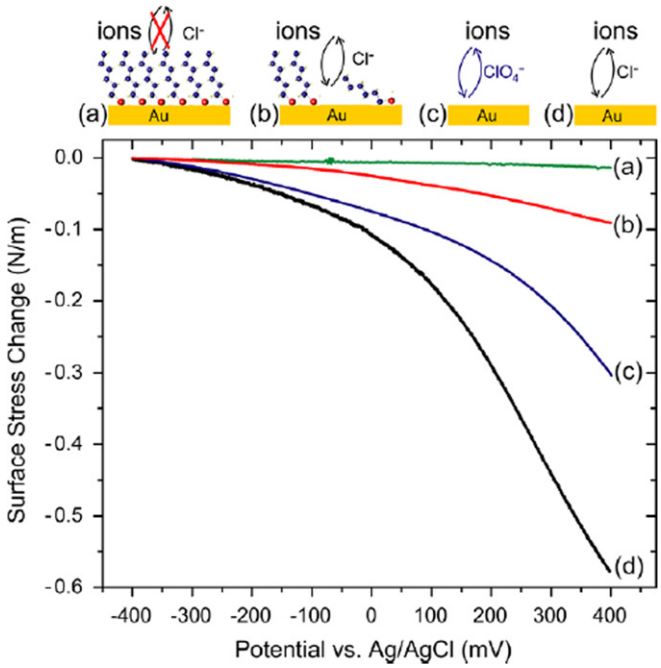

Figure 7. A large cantilever deflection is seen as the surface potential of a cantilever is increased from −400 mV to +400 mV versus Ag/AgCl. There are anions present in the surrounding buffer that can come into contact with the gold-coated cantilever. The situations (a)–(d) show that larger deflections are seen when the anions have more easy access to the surface. (c) and (d) compares the effect of ClO_4^- and Cl^- anions attracted to a pure gold surface [74].

In 2009, Arroyo-Hernández *et al* [78] introduced another feature that is critical to control when using a gold anchoring layer: the charge state. They investigated the resulting cantilever deflections arising from thiolated DNA strands binding to gold. The gold coating on the cantilevers was deposited using either e-beam deposition or resistive heating.

Table 1. Summary of experimental findings with respect to the origin of surface stress.

Year	Reference	Argument	System studied
2000	[19]	Electrostatic, steric and hydrophobic	DNA in saline sodium citrate hybridization buffer
2001	[70]	Interplay between configurational entropy and inter-molecular energetics	DNA in sodium phosphate buffer
2002	[71]	Electrostatic and steric hindrance effects	DNA in triethyl ammonium acetate buffer
2005	[80]	Electrostatic (and entropic, hydrophobic, hydration and solvation surface forces)	DNA in saline sodium phosphate buffer
2006	[72]	Electrostatics, ionic hydrogen bonds. The effect of counter ions from aqueous solution	Thiolated alkanechains in sodium phosphate buffer
2008	[79]	Hydration forces in between ss-DNA or ds-DNA	DNA in saline sodium phosphate buffer
2010	[74]	Intermolecular electrostatics, Lennard-Jones interactions, the effect of adsorption-induced changes in the electronic density of the metal film combined with the associated electronic charge transfer from the gold to the thiol bond	Thiolated alkanechains deposited from deposited from the gas phase

It was seen that e-beam deposition results in compressive stress whereas resistive heating deposition results in tensile stress. Furthermore, the effect of grounding the gold-coated cantilever during immobilization was investigated. The surface stress of the cantilever coated with gold using resistive heating changed from tensile to compressive when the cantilever was grounded. The topography of the two gold films were similar and the authors conclude that the critical feature must be the charge state of the gold film that makes the DNA strands arrange themselves differently depending on the interaction of the phosphate back-bone and the gold layer.

2.2.3. Surface stress measurements—hydration forces. In 2007, an idea proposed by Hagan *et al* in 2002 [67] was tested experimentally by the group of Tamayo [79]. The theoretical proposal suggests that hydration forces have a large impact/significance on the generated surface stress. The experiments show that both ss-DNA immobilization and DNA hybridization can be measured with high accuracy (fM concentrations) by simply observing the cantilever deflection as the relative humidity of the environment is alternated between 0% and 100%. The behaviour of a ss-DNA layer and a ds-DNA layer as a function of humidity is drastically different. Therefore the effect can be used to detect hybridization.

2.2.4. Surface stress measurements—conclusions. In conclusion, many experimental conditions influence the surface stress generation and great care has to be taken in design and interpretation of experiments. A summary of experimental findings with respect to the origin of surface stress is given in table 1. Issues such as gold coating of the cantilever, which at first seems very straightforward, have been seen to have large influence on the signal generation. More fundamental investigations are needed in order to fully understand the origin of surface stress. By understanding and controlling the many factors contributing to the generation of surface stress it will be possible to find ways of enhancing sensitivity and reliability of the signal. Naturally, reference cantilevers that can eliminate responses due to external factures such as temperature variations or buffer changes should be utilized.

2.3. Detection of effects related to bulk stress changes

The considerations on surface stress changes only apply when the thickness of the thin film on the top of the cantilever is much smaller than the thickness of the cantilever itself. In several applications stress is generated in the bulk of the cantilever material(s) whereby the signal interpretations as well as the general applications are different. Bulk stress changes can, for example, be applied in temperature sensing utilizing bi-material cantilevers. Using strings, volume changes in a single material are easily detectable.

2.3.1. Bi-material cantilever. Bi-material cantilevers consist of two material layers with different expansion coefficients α_1 and α_2. If such a bimorph cantilever is exposed to a changing influence parameter (i.e. temperature or humidity), named X, and X_0 is the initial parameter value, the cantilever bends. The tip deflection of a bi-material cantilever is given by [81–83]

$$\Delta x(X) = \frac{3L^2}{h_2^2}\left[\frac{(h_1+h_2)}{3\left(1+\frac{h_1}{h_2}\right)^2+\left(1+\frac{h_1\widehat{E}_1}{h_2\widehat{E}_2}\right)\left(\frac{h_1}{h_2}+\frac{h_2\widehat{E}_2}{h_1\widehat{E}_1}\right)}\right] \times(\alpha_1-\alpha_2)(X-X_0), \tag{2.23}$$

where h_1 and h_2 are the thicknesses and $\widehat{E}_1$ and $\widehat{E}_2$ the corresponding Young's moduli of the two material layers. The bending response of a bimorph cantilever can be optimized by choosing the right thickness corresponding to equation (2.23). The two materials need to have different expansion coefficients with respect to the parameter/analyte to be detected and should be chosen carefully in order to optimize sensitivity. The best known application of bi-material cantilevers is as thermal sensors where two materials with different thermal expansion coefficients are used [81, 84, 85]. Bi-material cantilevers can also be used as chemical [82, 86] and humidity sensors [3, 87]. If the sensitive layer is significantly thinner than the structural layer, the bending behaviour can be approximated by Stoney's equation (2.21).

2.3.2. Volume changes measured with strings. The eigenfrequency of strings is mainly defined by the tensile stress in the string material and is given by (2.7). If the volume of the string material expands due to an external changing parameter, the strain in the string is released which results in a resonant frequency shift. Assuming the volume expansion to be a linear function of an external parameter X, the total strain in the string can be written as

$$\varepsilon(X) = \varepsilon_0 - (\alpha_{\text{str}} - \alpha_{\text{sub}})(X - X_0), \tag{2.24}$$

where ε_0 is the initial pre-strain of the string, α_{str} and α_{sub} are coefficients of a specific length expansion of the string material and the substrate material, respectively. In a specific application α_{str} and α_{sub} represent, e.g., the coefficient of thermal expansion or the coefficient of humidity-induced volume expansion. Assuming that Young's modulus E is not a function of X, the stress in the string becomes

$$\sigma(X) = \sigma_0 - \upsilon(\alpha_{\text{str}} - \alpha_{\text{sub}})(X - X_0) \tag{2.25}$$

with the pre-stress σ_0. The eigenfrequency of a string is then given by [38]

$$\omega_n(X) = (n\pi)\frac{1}{L}\sqrt{\frac{\sigma_0 - \widehat{E}(\alpha_{\text{str}} - \alpha_{\text{sub}})(X - X_0)}{\rho}}. \tag{2.26}$$

The sensitivity of a string-based sensor can consequently be optimized by choosing stiff string and substrate materials with a large difference in their volume expansion behaviour. In the case of using polymeric strings on a glass substrate the difference in the swelling due to moisture is large, since the water absorption of the polymer is relatively high and the water uptake of glass can be neglected. For SU-8 strings a relative humidity resolution of 0.006% [88] has been achieved. Temperature also causes the string material to expand. Resonant AuPd micro-strings have been successfully used as temperature sensors [89].

3. Sensor materials and fabrication

Basically, cantilevers are fabricated in either silicon- or polymer-based materials. Examples of the two types of cantilevers are shown in figure 8. Although the design of the sensors is similar, the schemes of fabrication are very different and will therefore be described separately below. In the majority of the research results published up to now, external optical read-out is used to measure the cantilever deflection. Therefore, the focus will be on the fabrication of simple free-standing beams suitable for optical read-out. In section 3.3, a short overview on the design and processing of more complex devices with integrated functionality is given. Independent of the cantilever material there are some requirements to the final cantilever structure.

(i) For increased surface stress sensitivity, the cantilever should be as thin and long as possible. This requires processing of suspended fragile structures.

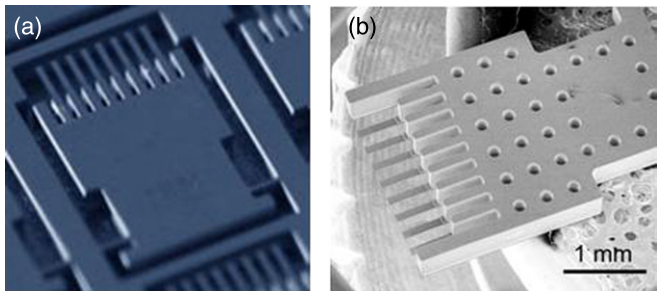

Figure 8. Scanning electron micrographs of silicon (*a*) and polymer (*b*) cantilevers. Both the chips have an array of eight cantilevers with a length of 500 μm and a width of 100 μm.

(ii) For mass sensing the clamping of the cantilever should minimize clamping losses. Furthermore, the material should have low internal damping and the cantilever geometry should allow for a high Q factor.

(iii) For all purposes the geometries of the cantilevers should be controlled with a high accuracy since the dimensions have a huge influence on the sensitivity and thus the uniformity of the sensors. For example, precise control of the geometries of reference and measurement cantilevers is crucial to avoid measurement errors.

(iv) For optical read-out, the surface of the cantilever needs to be reflecting and of high optical quality. The surface should not be rough and thereby scatter the light in all directions.

(v) The cantilevers should ideally have no initial bending. Initial bending complicates the optical alignment and makes the cantilevers more prone to spurious signals due to changes in temperature, refractive index, etc.

3.1. Silicon-based devices

3.1.1. Materials. Silicon-based materials are predominantly used for the fabrication of cantilever sensors. Silicon microfabrication is well established and uses technologies initially developed by the IC industry in the 1960s. Hence, integration of wiring for actuation and read-out is quite straightforward. Materials such as silicon, silicon nitride and silicon oxide are also well characterized and stable over time. As a consequence, cantilevers fabricated with these classical materials can be operated in a large range of temperatures and environmental conditions. Microcantilevers are typically around 1 μm thick and 450–950 μm long. Highly sensitive cantilevers with thickness $h = 500$ nm and length $L = 500$ μm are commercially available [90, 91] and ultrathin cantilevers with $h < 200$ nm have been fabricated [92, 93].

3.1.2. Bulk micromachining. It is impossible to realize advanced mechanical structures with micrometre dimensions using fine mechanics. Instead, cleanroom-based processes are used where the cantilevers are fabricated by etching three dimensionally in a silicon wafer. A typical strategy for realization of silicon-based cantilevers consists of three main steps illustrated in figure 9: (*a*) substrate preparation, (*b*) cantilever patterning and ((*c*), (*d*)) device release. This

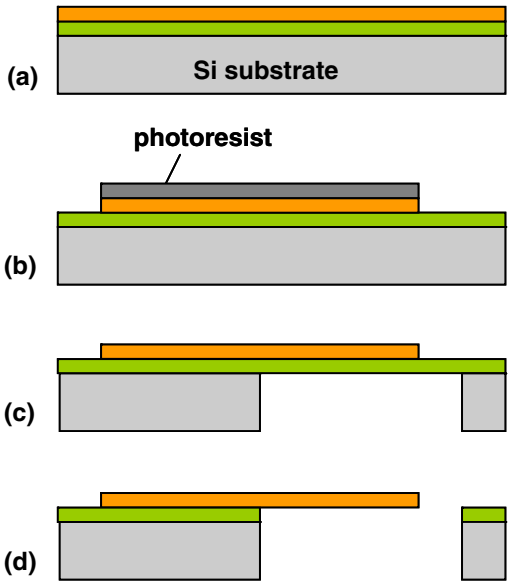

Figure 9. Fabrication of silicon-based cantilevers by bulk micromachining: (*a*) substrate preparation by thin film deposition; (*b*) patterning of cantilevers by photolithography and etching; (*c*) cantilever release by etching through the bulk wafer from the backside and (*d*) removal of the etch stop layer.

approach, where the suspended structures are defined by etching from the backside all the way through the wafer, is called bulk micromachining [94].

The fabrication is based on single crystal silicon wafers with thicknesses of 350–500 μm. During substrate preparation thin films of the actual cantilever material such as silicon nitride, silicon oxide or poly-silicon are deposited. The thickness of these films defines the final thickness of the cantilevers. Usually, a three-layered substrate is prepared, see figure 9(*a*), where the intermediate material is the so-called etch stop layer. This material protects the actual device layer during the release in order to secure a well-defined thickness and a highly reflecting surface of the cantilever. A common method is the use of single crystal silicon wafers (1 0 0) with a built-in silicon oxide film. These wafers are also called silicon-on-insulator (SOI) and can be ordered from a range of suppliers [95–97]. The cantilevers are defined by UV patterning of photoresist [98] on the front side of the wafer. For nanoscale cantilevers, the UV lithography can be replaced by electron-beam lithography [99]. The resist pattern is transferred to the device layer by wet etching [98] or reactive ion etching (RIE) [98], figure 9(*b*). The etching from the backside is achieved with potassium hydroxide (KOH) [98] or by deep reactive ion etching (DRIE) [100], figure 9(*c*). As a final step the etch stop layer is removed to release the cantilevers, figure 9(*d*).

The process results in free-standing cantilevers, accessible from both sides of the wafer. This is often advantageous. Both sides of the cantilever can be easily inspected and the cantilever can be placed in a liquid or gas flow perpendicular to the cantilever where the etched holes in the wafer serve as microfluidic channels. However, the cantilevers are rather fragile and not well protected. Moreover, etching through the entire silicon wafer is time consuming.

In recent years, materials such as silicon carbide [101], graphene [102] and diamond-like carbon [103] have emerged as alternatives to silicon, all offering unique chemical and mechanical properties.

3.2. Polymer-based devices

3.2.1. Materials. Since the late 1990s, an increasing amount of work has been reported on the fabrication of polymer-based cantilevers. The main motivation to introduce polymers is that Young's modulus typically is two orders of magnitude lower than for traditional silicon-based materials. Consequently, the stiffness of the cantilevers is reduced and the sensitivity increases. Equation (2.19) shows that the cantilever bending due to surface stress changes is directly proportional to Young's modulus of the cantilever material. The increased sensitivity is achieved if the thickness of the polymer cantilevers is comparable to the ones fabricated using silicon. Another important driving force to evaluate various polymers and fabrication methods is the possibility to reduce costs of raw material and fabrication.

In 1994, Pechmann and co-workers fabricated the first polymer microcantilevers with a standard Novolak-based photoresist as cantilever material [104]. In 1999, Genolet used the negative epoxy photo-resist SU-8 to define AFM-cantilevers [105]. Young's modulus of SU-8 is low (around 4 GPa [106]) compared with silicon and silicon nitride (180 and 290 GPa, respectively) which makes it a suitable candidate for micromechanical structures for surface stress measurements [107, 108]. In parallel, a large number of well-known polymers such as polyimide [109, 110], polystyrene [111–113], polypropylene [113], polyethylene therephtalate (PET) [114] and fluoropolymer [115] have been evaluated for the fabrication of micromechanical sensors. Recently, new thermoplasts specifically developed for microfabrication such as parylene [116, 117] and TOPAS® [118, 119] were introduced as cantilever materials.

3.2.2. Surface micromachining. A typical process scheme for the fabrication of polymer cantilevers is illustrated in figure 10. Compared with silicon-based devices, the free-standing structures are fabricated by building up layers on the surface of a carrier substrate. This approach is called surface micromachining [120]. First, a so-called sacrificial layer is applied, figure 10(*a*), followed by deposition of a thin cantilever material. In most cases this is achieved by spin-coating an organic solution of a polymer. An interesting alternative is parylene, which is deposited by chemical vapour deposition using di-para(xylylene) [121].

The most straightforward method to pattern the polymer cantilever is to use UV-photolithography, figure 10(*b*). This requires that the polymer is a photoresist such as SU-8 or polyimide [105, 107–109]. The thin polymer film defining the cantilevers is spin-coated, baked and exposed using standard equipment, which minimizes fabrication time and costs. An alternative approach is patterning the cantilevers by a combination of traditional photolithography and polymer etching. For example, O_2-plasma etching has been used

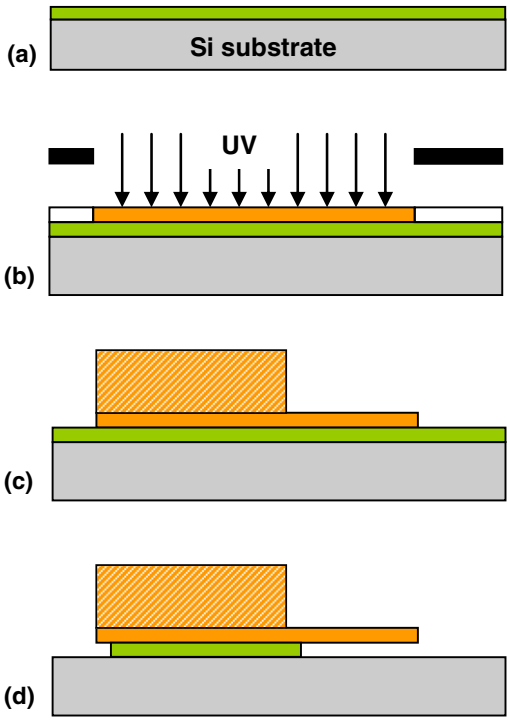

Figure 10. Fabrication of polymer cantilevers by surface micromachining: (*a*) deposition of sacrificial layer; (*b*) patterning of cantilevers by direct UV lithography; (*c*) definition of chip body; (*d*) cantilever release by partial or complete etching of the sacrificial layer.

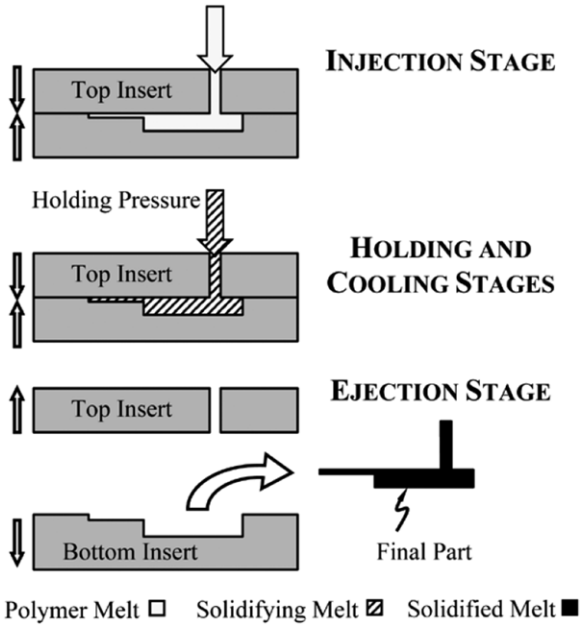

Figure 11. Illustration of the injection moulding process [113].

to define micromechanical sensors in parylene [117] and polyimide [122]. Another promising method of polymer patterning, eliminating some limitations on material selection, is nanoimprint lithography (NIL) [123, 124]. Recently, the fabrication of 4.5 μm thin cantilevers by NIL was demonstrated [118]. As alternatives to cleanroom-based patterning methods, laser ablation [114] and micro-cutting [111] have been suggested. So far, these approaches present major drawbacks in terms of chip contamination, precision and reproducibility.

After definition of the cantilevers in the actual device layer, a polymer chip body can be added on top to facilitate handling of the cantilevers after device release. For example, subsequent steps of SU-8 photolithography have been used to pattern a chip body with a thickness of several hundred micrometres, figure 10(*c*) [105]. With this approach, direct integration of SU-8 cantilevers in complete microfluidic systems has been shown [125]. Alternatively, a PDMS block can be defined on top of polymer cantilevers [120].

Finally, the cantilevers are released from the frontside of the wafer. The sacrificial layer immediately below the cantilever is removed by a selective etch resulting in a cantilever which is suspended some micrometres above the silicon substrate, figure 10(*d*). Both wet etching [38, 126–130] and dry etching in a plasma [131, 132] are possible. Underetch rates are often quite low as the access of the etchant to the sacrificial layer is restricted, resulting in long processing times. Furthermore, due to the small spacing between the substrate and the cantilever the risk of adhesion of the cantilever to the substrate increases and the phenomena called stiction might occur [133]. The risk of stiction is to some degree minimized by using dry etching for cantilever release. Alternatively, anti-stiction coatings can be used as release layers [134–136].

3.2.3. Three-dimensional microfabrication. Some interesting alternatives to the classical surface micromachining approach were introduced for the fabrication of micromechanical sensors. McFarland *et al* reported thermoplastic injection moulding (micro-moulding) of cantilevers using polystyrene, polypropylene and a nanoclay polymer composite as illustrated in figure 11 [112, 113]. Other, more serial patterning methods such as laser ablation [114], microstereolithography [137] and multi-photon-absorption polymerization [138] have been explored. These methods appear as expensive alternatives to injection moulding, but they present a high degree of freedom for design of prototypes. For example, the definition of polymeric nanometre-sized cantilevers should be possible.

3.2.4. Challenges and perspectives. Fabrication of polymer-based micromechanical devices is still in an early phase and many issues need to be solved before robust and stable cantilevers can be routinely fabricated. One of the main challenges using polymer chips for mechanical sensing is the stability of the devices during measurements. Moisture absorption in liquids or degassing in vacuum results in drift of the output signal [139]. Schmid *et al* showed that a change in air humidity is reflected in a shift of the resonant frequency of SU-8 cantilevers due to water absorption [140]. Other phenomena such as creep deformation, ageing or bleaching can affect the long-term stability of cantilevers. To some extent, process optimization can minimize drift and increase time-stability [130, 141].

For thin polymer cantilevers, reflectivity is insufficient for optical read-out and therefore a metal coating is required. Furthermore, gold coatings are typically used as linker surfaces for the attachment of receptor molecules. The deposition of metals is a critical step as it implies the use of elevated temperatures. This heavily affects the stress gradients in polymer cantilevers [142]. A possible solution is direct surface functionalization of polymer cantilevers, avoiding gold layers as binding interfaces [143, 144]. The laser reflection can be ensured by only integrating a small metal pad at the apex of the cantilever.

Since the introduction of polymers for the fabrication of cantilever sensors, the spring constant has been continuously reduced. The fabrication of 2 μm thin SU-8 cantilevers with $L = 500\,\mu$m and low initial bending is possible [141]. This is promising in terms of sensitivity, but at the same time the reduction in the thickness implies an amplification of the aforementioned instabilities during measurements. For most applications, polymer cantilevers with a thickness of 5 μm are more than suitable for surface stress measurements. Instead of trying to further increase sensitivity by decreasing the cantilever thickness, the focus should be on improving control of stability.

In the future, the improvement of new fabrication methods such as NIL or injection moulding could allow the selection of new polymer materials which are less affected by the measurement conditions. In parallel, fabrication costs could be significantly reduced.

3.3. Cantilevers with integrated functionality

Fabrication becomes more complicated when read-out of the cantilever bending and/or additional features such as electrodes or heater elements are integrated into the structure. Here the integration of piezoresistive read-out is described as an example. The details of this read-out method are discussed in section 4. Other examples are the integration of metal electrodes for electrochemistry [145] and thermal actuation [146].

In piezoresistive cantilever sensing each cantilever has an integrated resistor which has piezoresistive properties. For silicon-based cantilevers, a silicon resistor is defined in microcrystalline or single crystal silicon and encapsulated in silicon nitride [147]. The silicon nitride serves as an efficient electrical insulation of the resistor and ensures that the device can be operated in liquids. The signal-to-noise ratio of the piezoresistive cantilever depends highly on the doping and the crystallinity of the silicon layer and the best performance is clearly found for single crystalline resistors [148]. The piezoresistive coefficient of doped silicon is high, resulting in very sensitive read-out. The cantilevers can detect deflections below 1 nm and the small size of the cantilevers makes it possible to realize a complete device with liquid handling and electronics on a few cm^2. In figure 12 an image of 10 cantilevers placed in a channel is shown. The channel is used to guide the liquids under investigation to the cantilevers [149].

Similar devices with integrated piezoresistive read-out can be realized in SU-8 [150, 151]. An example of two polymer cantilevers with integrated gold resistors is shown in figure 13. The gold resistors serve as low noise piezoresistors and the signal-to-noise ratio is comparable to the value for the silicon nitride cantilevers with single crystal resistors [152] due to the much lower electrical noise in gold compared with silicon. The relative resistance change of gold is approximately 40 times smaller than for single crystal silicon and new materials are therefore being investigated as possible candidates for even better piezoresistors.

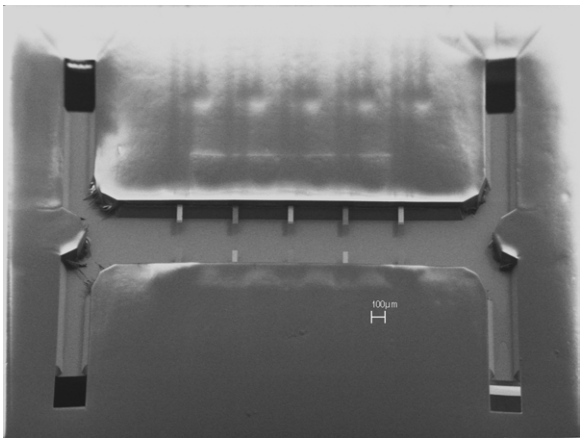

Figure 12. Scanning electron microscope image of 10 silicon nitride cantilevers with integrated silicon piezoresistors in a channel. The channel has two inlets and two outlets. Every second cantilever is coated on the top side with a 20 nm thick gold layer for surface functionalization. These cantilevers appear brighter.

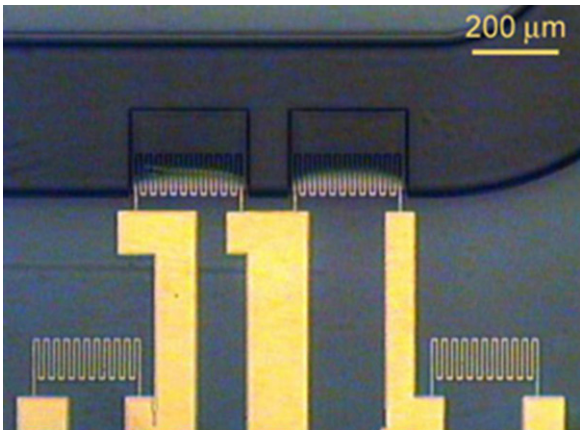

Figure 13. Optical microscope image of two polymer cantilevers with integrated gold resistors placed in a channel. Two additional gold resistors can be seen on the body of the chip.

Several groups have synthesized composite materials by mixing nanoparticles into polymers. The availability of conductive [153, 154], magnetic [155] and luminescent [156] polymers for cantilever fabrication allows adding functionality to the devices. For example, composites of carbon nanoparticles and SU-8 were used to fabricate cantilevers with integrated polymer piezoresistors [157]. There, the challenge is to find a material which is soft and at the same time has a large resistance change upon deflection. Moreover, the electrical noise in the system should be low. Materials such as polyaniline [158], 3,4-ethylenedioxythiophene (PEDT) [159]

Table 2. Comparison of cantilever materials and fabrication methods.

Material	Si[a]	SiN[b]	SiO[c]	SU-8	Topas	Polystyrene
Cantilever fabrication						
Fabrication method	Etching	Etching	Etching	UV	NIL	Injection
Fabrication costs	High	High	High	Medium	Medium	Low
Influence of metal coating deposition	None	None	None	Bending	Bending	Bending
Cantilever properties	*Theoretical values based on typical dimensions* ($L = 500\,\mu$m, $w = 100\,\mu$m)					
Thickness h	500 nm	500 nm	1 μm	2 μm	4.5 μm	5 μm
Youngs'modulus E	180 GPa	290 Gpa	85 GPa	4 GPa	2.6 GPa	3 GPa
Poisson's ratio ν	0.28	0.27	0.25	0.22	0.26	0.34
Density ρ	2.3 g cm^{-3}	3.0 g cm^{-3}	2.7 g cm^{-3}	1.2 g cm^{-3}	1.0 g cm^{-3}	1.0 g cm^{-3}
Spring constant k	4.5 mN m	7.3 mN m	17.0 mN m	6.4 mN m	47.4 mN m	75.0 mN m
Resonance frequency f_o ($f_o = \omega_o/2\pi$)	2.8 kHz	3.2 kHz	3.7 kHz	2.4 kHz	4.6 kHz	5.5 kHz
Surface stress sensitivity $\Delta z/\Delta\sigma$	12.0 m^{2}N^{-1}	7.6 m^{2}N^{-1}	6.6 m^{2}N^{-1}	36.6 m^{2}N^{-1}	10.5 m^{2}N^{-1}	6.6 m^{2}N^{-1}
Mass responsivity $\Delta f/\Delta m$	24.4 Hz ng^{-1}	21.2 Hz ng^{-1}	13.8 Hz ng^{-1}	10.0 Hz ng^{-1}	10.1 Hz ng^{-1}	10.6 Hz ng^{-1}
Measurements	*Qualitative comparison of sensor performance*					
Damping (quality factor Q)	Viscous	Viscous	Viscous	Material	Material	Material
Thermal stability	High	High	High	Medium	Low	Low
Moisture absorption in bulk	Low	Low	Low	High	Medium	Medium
Time-stability	Years	Years	Years	Months	Months	—
Reflection of optical beam without metal	High	High	High	Low	Low	Low

[a] Crystalline Si.
[b] LPCVD nitride.
[c] PECVD oxide.

and SU-8 doped with 20 nm carbon particles [157, 160] have been investigated.

3.4. Comparison of materials and fabrication methods

In table 2, key parameters for cantilever sensors are compared. For a specific application, it is important to consider advantage and drawback of the various materials and fabrication methods discussed.

For detection of mass changes (dynamic mode) elaborated in section 2.1, silicon-based materials are in general preferred. There, the lower internal damping is the main reason for a higher quality factor of the devices. Also, the higher Young's modulus and the availability of nanopatterning methods such as e-beam lithography open up for the fabrication of nanometre-sized cantilevers with high resonant frequency and increased mass sensitivity. Polymer cantilevers can be used in dynamic mode, but here the material damping is significant and factors such as temperature and humidity directly influence the measurements.

For measurement of surface stress in liquids, silicon-based materials are well suited as drift due to moisture absorption in the bulk can be neglected. On the other hand, a considerable response to charge accumulation upon changes in pH has been reported [161]. Furthermore, the beam thickness has to be pushed to the limits of what is possible in microfabrication to achieve high surface stress sensitivity. Therefore, polymer cantilevers present a good alternative due to the increased flexibility. Some authors directly compared polymer- and silicon-based cantilevers in surface stress measurements. In general, the performance of polymer devices is comparable to their silicon-based counterparts [47].

For sensor operation at elevated temperature (e.g. in calorimetry), silicon-based cantilevers are superior to the ones made of polymer due to the increased temperature stability. Finally, fabrication using silicon-based materials is in general more expensive than using polymers.

4. Sensor read-out principles

In order to detect minute deflection of cantilevers and related structures different sensitive displacement sensors have been investigated. Some methods are robust and well established but rather bulky, whereas other techniques are a bit more immature but with the promise of becoming miniaturized. The presented read-out methods are summarized in table 3.

4.1. Optical read-out

Today, optical leverage is the commonly used read-out system. A laser is focused on the back of the cantilever which acts as a mirror. The reflected laser light is detected by a position sensitive photodetector. The technique routinely gives a resolution of 1 nm deflection and even sub-angstrom

Table 3. Summary of read-out methods.

Read-out method	Pros	Cons	Used in	Company
Optical leverage	Simple read-out method, known from AFM; can be used on any cantilever with a good optical quality	Difficult to apply for large arrays; prone to optical artefacts such as change in refractive index; not suitable for nanometre-sized cantilevers	Surface stress; mass; bulk stress	Concentris, Veeco
Capacitive	Useful for nanometre-sized cantilevers; read-out does not affect the mechanical properties of the cantilever	Stray capacitances make pre-amplifications and CMOS integration necessary; this complicates the fabrication	Mass	—
Piezoelectric	The principle can be used for actuation as well as read-out	Many piezoelectric materials are not cleanroom compatible; many piezoelectrical materials are only suitable for dynamic measurements	Surface stress; mass; bulk stress	Intelligent Microsystems Center
Piezoresistive	Facilitates large arrays and system integration; works in all media and in all modes of operation	A piezoresistive layer needs to be integrated into the cantilever which affects the mechanical performance; for operation in liquid, care has to be taken in order to insulate the resistor	Surface stress; mass; bulk stress	Nanonord, Seiko
Hard contact	Offers a 'digital' read-out where a signal is only generated when the cantilever is in resonance; high signal-to-noise ratio	Wear of the counter electrode is a challenge; works only in air	Mass	—
Tunnelling	Potentially very sensitive detection of cantilever bending	Complicated operation and only works in air	Mass	—
Integrated optical methods (waveguides)	Suitable for large scale arrays with the same sensitivity as optical leverage	More complicated fabrication and packaging; prone to optical artefacts, such as changes in refractive index	Surface stress	—
Autonomous devices	Simple device concept with no need for external energy	Difficult to realize the device such that there is no leakage of dye molecules	Surface stress	—

resolution can be achieved. However, this set-up does not facilitate the simultaneous read-out from a reference cantilever. To allow for the detection of multiple cantilever deflections simultaneously new optical read-out schemes have been developed. In a solution originally developed at IBM, Zürich [18, 162, 163], an array of eight commercially available VCSELs (vertical cavity surface emitting lasers) is used to illuminate eight cantilevers spaced with the same pitch (250 μm) as the individual VCSELs. The reflected light is collected by a single photodetector. The photodetector can track the individual movement of the spots reflected from each respective cantilever. This concept is now the platform in the commercially available system from Concentris [90]. A different approach has been developed in the group of Arun Majumdar at Berkeley, USA. There, a two-dimensional array of cantilevers is illuminated simultaneously with an expanded and collimated laser beam. Each cantilever only reflects the light from a mirror placed at the apex. The resulting two-dimensional arrays of reflected spots are captured by a high resolution CCD camera [164–166]. The movement of the individual spots can be registered with a resolution of 1 nm and read out from two-dimensional cantilever arrays with about 720 cantilevers has been reported using this technique. The technique is simple to instrument, however the optics is, in its present form, bulky and the resolution is less than for the optical leverage technique—being limited by the resolution of the CCD array.

In some cases, especially in more fundamental studies of, for example, signal generation, information on the bending profile of the full cantilever is advantageous. One possibility is to scan a laser across a single cantilever and monitor the deflection as a function of cantilever position. A line profile of the cantilever can then be obtained [167]. A full field deflection picture can be obtained using interferometric imaging methods [168]. Thereby it is possible in real-time to monitor the deformation of the full cantilever surface. Such studies have shed new light on the cantilevers mechanical response to surface stress changes [167] and charge distributions on the cantilever surface [169].

Recently, new ways of realizing potentially extremely compact and sensitive sensor systems have been published. One possibility is to place the cantilever above a VCSEL and use the cantilever to create a so-called external cavity between the laser and cantilever. The light reflected back into the VCSEL creates a self-mixing interference signal [170]. Thereby a deflection resolution of less than 1 Å can be achieved and large arrays can be realized using sandwiched two-dimensional VCSEL and cantilever arrays.

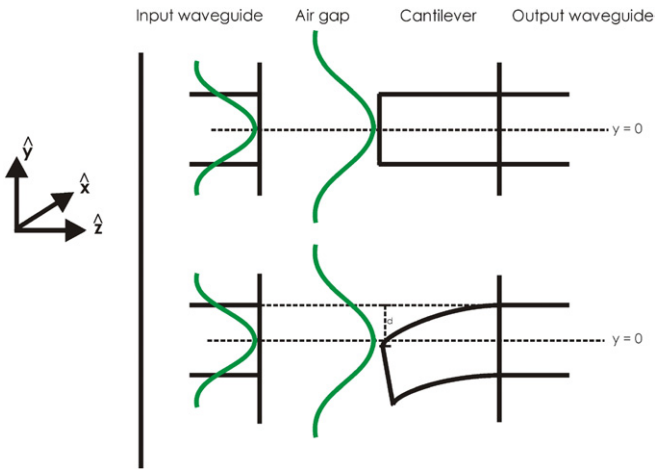

Figure 14. Schematic drawing of a cantilever-waveguide read-out principle. As the cantilever deflects, less light can couple across the air gap and into the cantilever-waveguide. This results in a decrease in the light intensity at the output waveguide. The drawing shows a homogeneous waveguide [174].

Alternatively, the optical read-out can be fully integrated. The first paper presenting an integrated optical read-out for use with microcantilevers was presented in 2006 by Zinoviev *et al* [171]. In the following two years, other groups presented similar systems [172, 173]. In all cases light is coupled into a cantilever-waveguide from one side and the intensity of the optical output is measured on the opposite side of the cantilever, see figure 14.

The cantilever is suspended across a channel with a width of 100–200 μm. As the cantilever-waveguide deflects, the intensity of the light coupled across the channel decreases due to a reduced overlap of the cantilever-waveguide and the output waveguide on the opposite side of the channel.

4.2. Capacitive read-out

Two electrodes separated by any material have a capacitance and this capacitance changes when the distance between the electrodes changes. If a cantilever is placed close to a parallel electrode the deflection of the cantilever will cause a capacitance change. This integrated read-out was first introduced for AFM probes [175, 176] and has later also been implemented in cantilever-based sensing. Today, capacitive read-out is mainly explored for mass detection in non-liquids. The sensor elements can be achieved by defining the cantilever in the top layer of an SOI wafer and using the buried oxide as a sacrificial layer to define the separation between cantilever and counter electrode [175, 177]. Alternatively, the device can be defined purely by surface micromachining using a design, where the counter electrode and the cantilever are defined simultaneously in the same device layer and the cantilever then deflects in the plane of the wafer [57, 178–183]. Such a design is illustrated in figure 15 where cantilever and counter electrode have been realized in one of the poly-silicon layers used in standard complementary metal-oxide-silicon (CMOS) fabrication. This design facilitates integration with CMOS technologies. Thereby integration with an IC is possible and signal processing close to the mechanical sensor can be achieved. These cantilever devices have resonant frequencies in the 1 MHz regime and a mass responsivity of 1 ag Hz^{-1} [179]. Recently, polymer walls have also been used as resonators with capacitive read-out and resonant frequencies of approximately 200 MHz and mass responsivities in the order of 0.1 zg Hz^{-1} in ambient air have been reported [184].

The capacitance changes are small, in the pF regime, and thereby they easily drown in stray capacitances in the system. Furthermore, capacitive read-out requires a high degree of process control since the surface quality of the cantilever and counter electrode as well as the spacing between them are crucial. Capacitive read-out has the advantage of offering an integratable read-out which does not influence the cantilever itself. No additional layer needs to be added with the risk of degrading the cantilevers' mechanical performance.

4.3. Piezoelectric read-out

Piezoelectricity has been widely used for both cantilever actuation and for detection of cantilever deflection. Basically, a mechanical stress generates an electrical potential across a piezoelectric material and vice versa. For high resolution detection of the deflection it is necessary to operate the cantilever in the dynamic mode since the voltage produced by a static force cannot be maintained by the thin film piezoelectric material. Thus, the piezoelectric read-out is primarily utilized in resonance mode. The first micromachined piezoelectric read-out was introduced in 1993 by Itoh and Suga [185–187]. In their work a piezoelectric zinc oxide film is deposited on one side of a cantilever and used for AFM. Other groups have pursued the use of piezoelectric read-out for AFM using either zinc oxide [188] or lead zirconate titanate (PZT) [189] thin films. Several groups are now implementing the same technique for cantilever-based sensing. For example, cantilevers originally designed for AFM have been used to monitor mercury in the ppb range [190] and the waterborn parasite *Giardia lamblia* has been detected using millimetre-sized glass cantilevers coated with PZT [191].

Silicon nitride cantilevers with PZT coatings have been developed by the group of Tae Song Kim and used for several years for biosensing. For example, detection of the PSA [192] and of Hepatitis B virus DNA [193] have been demonstrated. Piezoelectric cantilever sensors are commercially available through the company Intelligent Microsystem Center [194].

Cleland *et al* have used aluminium nitride as a piezo-electrical material [195]. Aluminium nitride is stiff and can be epitaxially grown on single-crystal silicon. Aluminium nitride is used in surface acoustic wave devices, and may prove useful for the integration of other types of mechanical devices as well. The material is cleanroom compatible and can be integrated with CMOS processing. Bridge resonators have been realized in aluminium nitride and fundamental resonance frequencies above 80 MHz have been reported. An example of aluminium nitride beams is shown in figure 16. In this early work the piezoelectric properties of aluminium nitride were not utilized. Instead the beams were actuated and read-out using a so-called magnetomotive technique [196]. Recently,

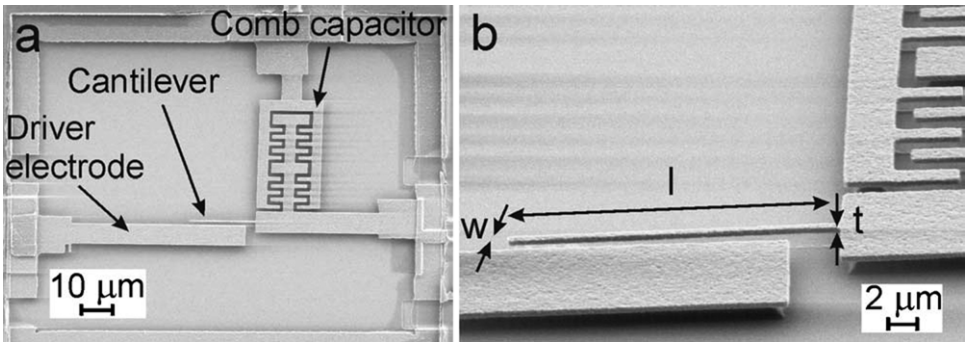

Figure 15. SEM images of fabricated poly-silicon cantilever structures on a CMOS chip. (*a*) Top view image of a defined cantilever structure. The cantilever is excited into lateral resonance by applying an ac and dc voltage between the driver electrode and the cantilever. The cantilever is connected to a comb capacitor in order to polarize the CMOS circuitry. (*b*) Tilted view image of a 20 μm long, 425 nm wide and 600 nm thick cantilever [179].

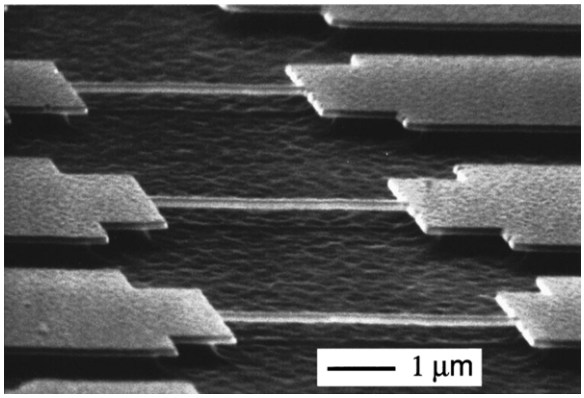

Figure 16. Series of four AlN beams, with undercut lengths ranging from 3.9 to 5.6 mm. The beams are 0.17 mm thick and the widths are 0.2 mm, increasing to widths of 2.4 mm at either end [195].

aluminium nitride cantilevers have been realized where the aluminium is sandwiched between two electrodes placed at the top and bottom of the cantilever. Thereby it is possible to drive the cantilever and to bias the cantilever with a dc current. It has been demonstrated that it is possible to tune the resonant frequency of the device with 34 kHz V^{-1} and the same piezoelectric layer has also been used for the read-out of the signal.

The challenge of this technique is that most piezoelectric materials are difficult to work with and they are not all cleanroom compatible. The read-out has the advantage of being easily scalable and with low power consumption. Cleanroom compatible materials such as aluminium nitride with a high stiffness and with interesting electrical properties will probably be further explored in the coming years.

4.4. Piezoresistive read-out

In piezoresistive cantilever sensing each cantilever has an integrated resistor which has piezoresistive properties. Due to the piezoresistive property the resistance changes when the cantilever bends. Thus, by an electrical measurement of a resistance change the deflection of the cantilever can be determined. The benefits of this method are that the principle works well in both liquid and gas phase and large arrays can be realized and read-out. Also, the technique is applicable for static as well as dynamic measurements. Sensing the cantilever deflection by integrating piezoresistors on the cantilever was initially developed by two groups for AFM imaging; Tortonese *et al* at Stanford University [197] and Rangelow *et al* at Kassel University [198]. AFM cantilevers with piezoresistive read-out are available through Seiko [199]. These cantilevers, originally optimized for AFM, have, for example, been used for the detection of thermal expansion in exotic new materials such as alpha uranium [200].

In 2000 the first cantilever-based sensing experiments using piezoresistive cantilevers were reported [20, 55]. Similar cantilever sensors have, since 2001, been commercially available through the company Cantion A/S. Here the cantilevers are placed in arrays of either 4 or 16. Such arrays have, for example, been used to monitor consolidated bioprocessing by detecting ethanol and glucose [201] and saccharide [202]. Recently, similar piezoresistive cantilever arrays have been developed and used for gas sensing [203].

Typically, a reference and a measuring cantilever are connected with two external resistors to form a Wheatstone bridge configuration [20, 204, 205]. In this way an output signal is only recorded when there is a difference in the deflection of the two cantilevers and the noise is reduced significantly. This measuring principle is shown schematically in figure 17.

Currently, several groups pursue the development of piezoresistive read-out [206, 207]. In the group of Pruit *et al* the read-out has been optimized for force sensing in living organisms and basic work on optimizing the read-out is conducted [208, 209]. The piezoresistive cantilevers can be integrated with CMOS for signal amplification and signal processing [210, 211].

In recent work, gold has been used as the integrated strain gauge. First for implementation in micrometre-sized polymer cantilevers [125, 150] and later for the realization of piezoresistive silicon carbide nanometre-sized cantilevers [33]. The small silicon carbide devices have been optimized and used for mass sensing. An impressive mass resolution of 1 ag is reported. Even though the gauge factor of gold is low the final mass resolution is high because of the low electrical noise in the gold film.

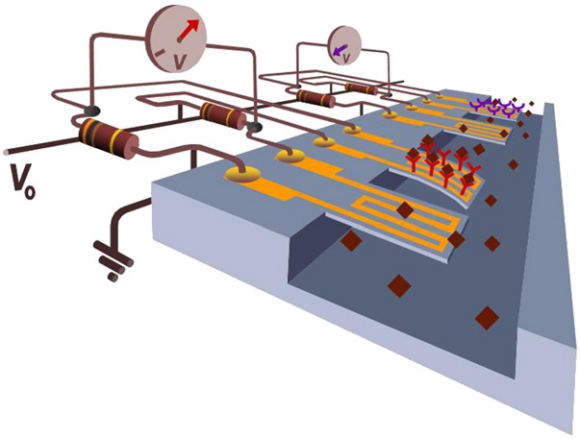

Figure 17. Schematic drawing of the cantilever measuring principle. When molecules attach to the cantilever, the cantilever bends and the bending is detected as a change in the resistance of the resistor placed inside the cantilever. A measurement is always performed on two cantilevers simultaneously. One cantilever serves as reference and only the differential signal is recorded (Daniel Häfliger).

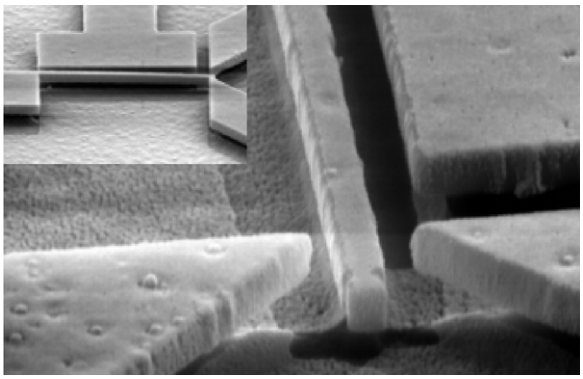

Figure 18. SEM image of a nanometre-sized cantilever designed for hard contact read-out (inset) and a close-up of the cantilever-electrode area. The cantilever (centre) is vibrated between the two sharp electrodes in front of the image. When in resonance the cantilever amplitude is large and it just touches the corners of the sharp electrodes. The current running between the cantilever and the sharp electrodes is monitored continuously and when a current signal is detected one knows that the cantilever is in resonance (Søren Dohn).

4.5. Hard-contact/tunnelling

One of the important parameters of a read-out system is the signal-to-noise ratio. One way to obtain a large signal-to-noise ratio is to use a system with a highly non-linear response to changes in deflection. Tunnelling and hard contact read-out are two such techniques. A tunnelling displacement sensor was used as the read-out system in the very first AFM [8] and in 1991 fully integrated on a chip to measure static cantilever deflections [212]. Recently, detection of resonant frequencies of nanoscale cantilevers has been performed by tunnelling [213, 214] and by hard contact read-out [215, 216].

In tunnelling read-out the cantilever is placed in close proximity to a counter electrode and the tunnelling current between the electrode and the cantilever is measured. The signal is, in principle, extremely sensitive but the fabrication and operation are complicated since very small electrode–cantilever gaps need to be realized. The gap spacing needs to be adjustable and the measured tunnelling current is in the pA regime which requires high-quality signal amplification. In hard contact read-out the cantilever is allowed to touch the electrode and the current (∼10 nA) running through the system is measured. The large current at resonance makes the read-out nearly digital and the quality of the signal amplification is not as important. An example of a hard-contact read-out device is shown in figure 18. The degradation of the contacts due to contamination is a drawback of the hard contact read-out method.

4.6. Autonomous devices

Inspired by the cantilever work a new sensor principle has emerged [142, 217]. Coloured marker molecules are loaded in a small volume closed by a flexible lid. The lid is coated with specific detector molecules, which bind the molecules under investigation. The binding of molecules causes the lid (just like a cantilever) to deflect and the marker molecules are released and can be detected by the naked eye. The complete sensor is approximately 1 cm × 1 cm in size and is fabricated

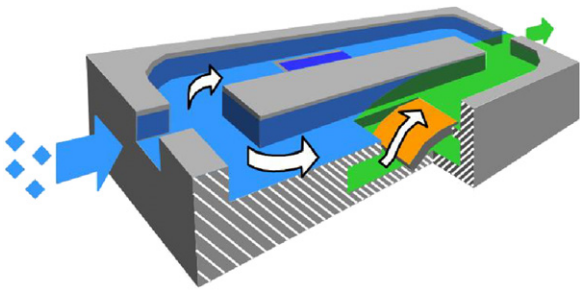

Figure 19. Schematic drawing of the operating principle of the 'lid' sensor. As molecules bind to the orange lid, the lid bends and releases the green colour (Daniel Häfliger).

in polymer. The deflection of the lid can also be caused by removal of a material on the top surface of the lid. The basic concept is illustrated in figure 19. So far the principle has been demonstrated by monitoring release of coloured marker molecules as aluminium is selectively removed from the top side of the lid.

4.7. Actuation

A variety of techniques have been implemented to actuate cantilevers and the choice of actuation method has to be coordinated with the read-out principle. In many experimental configurations the cantilever is actuated by the use of an external piezoelectric platform on which the cantilever chip is mounted and the whole chip is vibrated at a given frequency. Alternatively, the actuation can be miniaturized and integrated with the sensor. Actuation principles include electrostatic actuation, thermal actuation and magnetomotive actuation. In electrostatic actuation an electrode close to the cantilever is biased with an alternating voltage with regard to the cantilever. This creates a periodic, electrostatic force on the cantilever. Electrostatic actuation has been used in combination with for example capacitive [179] and hard contact read-out [57]. Electrostatic actuation can be used with dielectric materials

such as silicon nitride or polymers where an inhomogeneous electric field produces a net force (Kelvin polarization force) acting on a dielectric micro- or nano-beam [128, 218–220]. In thermal actuation a bimorph cantilever is heated in a pulsed manner using for example an integrated resistive heater [221] or an external laser [222]. Also, natural thermal vibrations due to fluctuations in the temperature of the structure can be used [223]. In magnetomotive actuation a static magnetic field is applied perpendicular to a cantilever through which an alternating current is running. The Lorentz forces will thereby cause the cantilever to deflect. The method requires large magnetic fields and low temperatures and has recently been used in mass detection using nanometre-sized cantilevers [224].

5. Applications

Examples of biomolecule detection have recently been presented in review papers [2, 7, 225] where levels of detections have also been compared. Also, the use of cantilever-based sensors in explosives detection has recently been discussed in a broader context [226]. Here some of the major research areas within cantilever applications will be described.

5.1. Surface functionalization

In order for a cantilever-based sensor to be able to detect specific molecules it needs to be coated with specific 'detector' molecules. For surface stress measurements it is important that only one side of the cantilever is coated since a uniform generation of surface stress on both cantilever sides will not result in a cantilever deflection. For mass sensing both sides can be functionalized although for maximum sensitivity it might be beneficial to have only the end of the cantilever functionalized. For all functionalization strategies the blocking of all other surfaces is crucial in order to prevent unspecific binding.

In order to selectively coat closely spaced cantilevers several different technologies have been developed. A common and widely used technology is to first coat the cantilevers with a thin gold layer on one side and then later use thiol-based chemistry to bind the probe molecules strongly to the gold surface. Within the cantilever community it is known that the quality of the evaporated gold has a high influence on the size and signature of the generated signals, as discussed in section 2.2.2. Great care has to be taken in preparing clean surfaces and also the crystallinity seems to have an effect on the signals. For silicon surfaces, silane coupling chemistry is often used and for polymer cantilevers new methods have been developed which, for example, use the epoxy groups on the surface of SU-8 [227]. Also, photo-activated chemistry which reacts with C–H bonds in polymers [143] has been utilized.

To expose different cantilevers in an array to different liquids one can apply microspotting using technologies developed for the realization of DNA arrays [228, 229]. Alternatively, capillaries placed with a spacing corresponding to the cantilever spacing are used as small beakers in which the cantilevers are inserted [90].

5.2. Bacteria detection

Whole bacteria or segments of bacteria can be caught directly on a cantilever. For example, if a cantilever is coated with antibodies against *E.coli* the cantilever will specifically bind to *E.coli*. The sensor might be expanded to contain several cantilevers each coated with a specific antibody. In this way it is possible to detect multiple bacteria simultaneously. One of the first groups to demonstrate bacteria detection was the group of Craighead *et al* which, in 2001, showed the mass detection of *E.coli* bacteria [223]. As more bacteria were bound to a cantilever the resonant frequency was seen to change correspondingly. Later the detection of *Salmonella enterica* was reported—in this case monitoring the change in surface stress upon binding of bacteria [230].

More fundamental studies have illustrated the influence of bacteria position on the generated mass signal [231, 232]. By analysing the resonant frequency shift for bacteria positioned at different positions along the cantilever and by operating the cantilever at different modes it was found that the mass signal depends on both the added mass and on the resulting change in stiffness of the cantilever as seen from equation (2.10). When a bacterium adsorbs on regions of high vibrational amplitude the resonant frequency change will be dominated by the mass changes. When the bacterium is positioned at a nodal point or at the clamped region the measured frequency response is governed by the change in stiffness. The addition of mass will thus result in an increase in the resonant frequency. These results highlight the necessity of controlling the position of bacteria absorption and show that either the stiffness effect or the mass change can be used for sensing purposes.

The growth of *E.coli* has been studied by coating cantilevers with a nutrient layer and monitoring the change in resonant frequency continuously [233] as the *E.coli* bacteria placed on top of the nutrient layer are growing. The resulting data show that it is possible to detect active bacterial growth in less than 1 h. Using rather large piezoelectric cantilevers made of PZT and glass (5 and 3 mm in length, 1.8 and 2.0 mm wide) the possibility of distinguishing between pathogen and non-pathogen *E.coli* was demonstrated [234]. The cantilever was coated with antibodies against pathogen *E.coli* and immersed in a mixed population of both pathogenic and non-pathogenic strains. The cantilever was seen to be highly selective only binding the pathogen species.

A highly sophisticated system for single cell detection has been developed by Manalis *et al*. Normally, resonators are damped when operated in liquid, thus lowering the sensitivity significantly. Manalis *et al* have removed this obstacle by flowing liquid inside the cantilever. Thereby, the device can be operated in a vacuum while analysing liquids inside the cantilever structure [235]. The first experiments focused on the demonstration of the detection of avidin binding. This was done by flushing the inner channel walls with biotinylated bovine serum albumin and subsequently monitoring the resulting resonant frequency shift as avidin is flushed through the system and binds to the functionalized walls. Single *E.coli* cell detection was demonstrated in 2007 [236]. Here a buffer solution containing *E.coli* is run

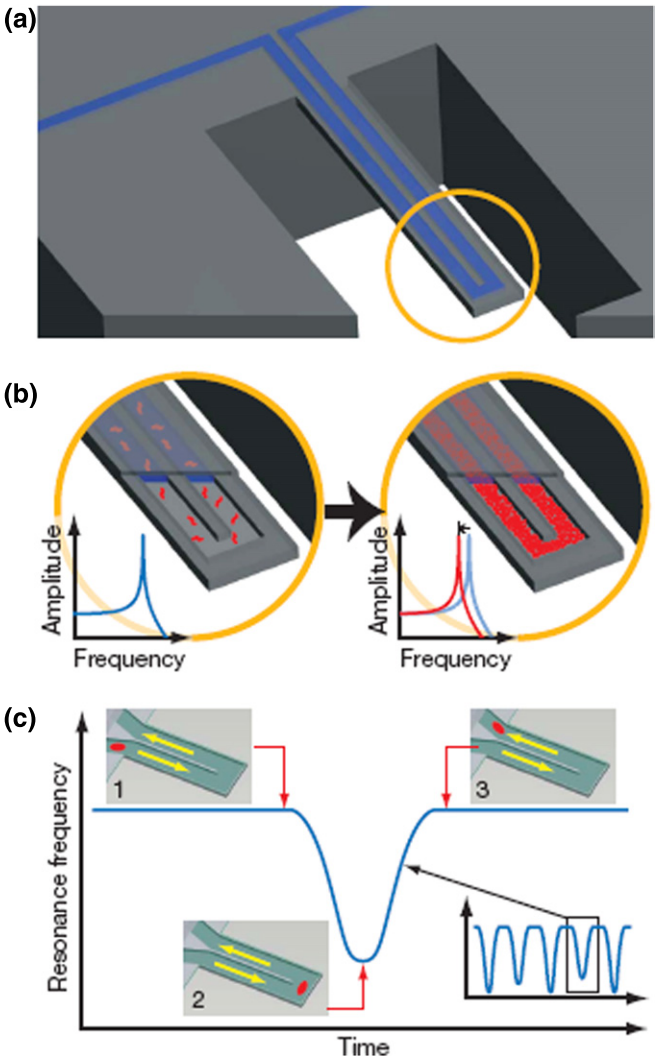

Figure 20. Schematic drawing of the principle of operation of a hollow cantilever. (*a*) A suspended microchannel translates mass changes into changes in resonance frequency. Fluid continuously flows through the channel and delivers biomolecules, cells or synthetic particles. Sub-femtogram mass resolution is attained by shrinking the wall and fluid layer thickness to the micrometre scale and by packaging the cantilever under high vacuum. (*b*) While bound and unbound molecules both increase the mass of the channel, species that bind to the channel wall accumulate inside the device, and, as a result, their number can greatly exceed the number of free molecules in solution. This enables specific detection by way of immobilized receptors. (*c*) In another measurement mode particles flow through the cantilever without binding to the surface, and the observed signal depends on the position of particles along the channel (insets 1–3). The exact mass excess of a particle can be quantified by the peak frequency shift induced at the apex [236].

through the system and the frequency response is measured continuously. The measured frequency changes are plotted in a histogram in order to find the mass distribution. The mass of an *E.coli* cell is found to be 110 ± 30 fg. A schematic of the device and its operation is shown in figure 20.

5.3. Point of care

As the cantilevers are label-free, potentially very sensitive and possible to integrate in portable systems they are often mentioned as a promising tool for POC diagnostics. One of the first examples of detection of clinically relevant proteins for diagnostics of prostate cancer was shown by the group of Majumdar *et al* [22]. Here, cantilevers were used to detect two forms of PSA over a wide range of concentrations from 0.2 ng ml^{-1} to 60 μg/ml in a background of human serum albumin and human plasminogen at 1 mg ml^{-1}. Antigen against PSA was immobilized using thiol chemistry on gold-coated silicon nitride cantilevers.

Microarrays that measure the expression levels of specific genes are today being developed for diagnostics. Methods that involve, for example, fluorescent labelling can achieve picomolar detection sensitivity, but they are costly, labour-intensive and time-consuming. Moreover, labelling with markers can influence the original signal. In 2006 it was demonstrated that cantilever sensors can be used to detect messenger RNA biomarker candidates in a solution of total cellular RNA [237]. The cantilevers were able to detect at the picomolar level without target amplification, and they were shown to be sensitive to base mismatches.

5.4. Drug discovery

In the field of drug discovery today, the study of membrane proteins is essential. Membrane proteins are important targets for new medicine. The group of Hegner *et al* [238] has recently shown that cantilever sensors can be used to study the interaction between specific membrane proteins and the bacteriophage T5. The bacteriophage is known to cause large structural changes in the cell upon binding. Subsequently the phage penetrates the cell and injects DNA. This binding event and the following conformational changes have been studied using cantilevers. In order to study the event, liposomes with specific membrane proteins have been realized and functionalized on one side of cantilevers by ink-jet spotting. The liposomes serve as simple cell membrane models. One of the results is shown in figure 21. A concentration of 3pM of T5 phages is exposed to the cantilevers and a clear shift in resonance is observed corresponding to an uptake of mass. When the cantilevers are subsequently exposed to a buffer the resonant frequency remains unchanged demonstrating the irreversible nature of the binding of the phages. This is the first time that membrane protein interactions have been studied in a microarray format and the cantilevers could be an interesting tool for drug screening as well as for measuring cells' mechanical response to drug treatments.

The growth of antibiotic-resistant superbugs such as methicillin-resistant *Staphylococcus aureus* (MRSA) and vancomycin-resistant *Enterococcus* has motivated studies on antibiotics and their modes of action. The bacteria's resistance to antibiotics can be caused by small changes in the bacteria cell wall and there is thus an interest in studies of the interaction between antibiotics and bacterial cell wall precursor analogues (mucopeptides). In the group of Mckendry *et al* the binding properties of the 'vancomycin' antibiotics have been investigated for vancomycin-sensitive and vancomycin resistant peptides [23]. It was possible to detecet vancomycin binding to peptide-coated cantilever arrays, with 10nM

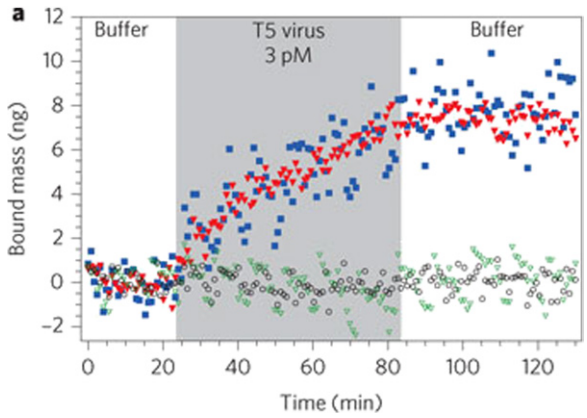

Figure 21. Measured change in mass of a cantilever exposed to T5 phages. The blue filled squares and red filled triangles correspond to two different measurements with liposome/membrane receptor coated cantilevers. The green open triangles and black open squares correspond to two negative controls where the cantilevers have been coated with casein [238].

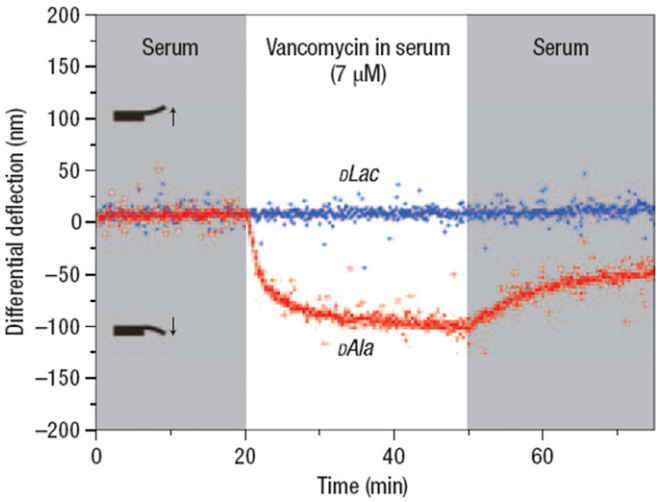

Figure 22. Measured differential cantilever deflection when vancomycin binds to vancomycin resistant peptides (DLAC) and to vancomycin sensitive (DAla) peptides [23].

sensitivity and at clinically relevant concentrations in blood serum. Also, from the measurements it was possible to quantify the binding constants for vancomycin-sensitive and vancomycin-resistant mucopeptides. Figure 22 shows the response from cantilevers coated with either vancomycin resistant peptides ((DLAC)) or vancomycin sensitive peptides ((DAla)). All measurements are differential and a polyethylene glycol (PEG)-coated cantilever is used as reference. The measurements are performed in serum and it is clearly seen that only the sensitive peptides bind the vancomycin.

5.5. Explosives detection

Cantilever-based sensors have been applied for trace detection of explosives. Such a miniaturized detector would be highly suitable for use in anti-terror efforts, boarder control, environmental monitoring and demining.

The sensing approaches either rely on specific receptors for binding of explosives or on specific properties of the explosives such as phase transitions. In the group of Thundat *et al* the explosives TETN and RDX have been detected in 10–30 parts-per-trillion levels using a gold-coated silicon cantilever functionalized with a SAM of 4-mercaptobenzoic acid [239]. The binding is semi-specific and recently Zuo *et al* have reported on increased specificity in the binding of TNT using a coating of 6-mercaptonicotinic acid (6-MNA) [240]. Here the measurements were performed using silicon oxide piezoresistive cantilevers.

Specific receptors for explosives detection are difficult to achieve and other receptor free possibilities have been explored. The cantilever can be highly sensitive to temperature changes and can thus be used for photothermal deflection spectroscopy [14]. When a material absorbs a photon, a fraction of the energy may be transformed into heat. A measurement of photothermal heating as a function of wavelength can provide an absorption spectrum of the material. The principle was first illustrated by Barnes *et al* [14] using a silicon nitride cantilever coated with a thin layer of aluminum. Heat changes of the order of picojoules were detected, in the investigation of, for example, fluorecein molecules. Later, the technique was applied in explosives detection [241, 242].

In another approach local differential thermal analysis (DTA) is used for the speciation of explosives. In DTA the material under study and an inert reference are made to undergo identical thermal cycles, while recording any temperature difference between sample and reference. As explosives are heated rapidly they will undergo decomposition and/or deflagration. These phase transitions can be used to achieve a thermal fingerprint of the explosives. Micrometre-sized cantilevers and bridges are ideal structures for DTA because of their low thermal mass. Micrometre-sized bridges with integrated heaters have been developed and used for the detection of explosives such as TNT, PETN and RDX [243–245]. The heater elements heat the bridge to around 600 °C. If explosives are present on the bridge these will start to evaporate or burn. In both cases the temperature of the bridge will change either because of evaporation or because of a local burning of explosives. This temperature change is measured by an integrated resistor which changes its resistance as a function of temperature change. The differential thermal response from bridges with and without adsorbed explosive vapour shows unique and reproducible characteristics depending on the nature of the adsorbed explosives. The method described is capable of providing unique signals for subnanogram quantities of adsorbed explosives within 50 ms.

5.6. Material characterization

Material characterization has always been an important issue in the field of microelectromechanical systems (MEMS). The properties of the used materials are process dependent and need to be known for a successful design. Standard mechanical material tests, such as the uniaxial tension test, to measure properties such as Young's modulus and fracture strength are not suitable for the characterization of thin film materials. The needed test specimens are very fragile and difficult to handle and align. A solution is to design

integrated micromechanical test structures such as membranes and cantilevers. By the use of equation (2.4) it is, for example, possible to extract Young's modulus from resonant frequency measurements—if the dimensions of the cantilever are known. Resonant microcantilevers have been used to determine Young's modulus of thin films since 1979 [246]. There exist a variety of other micromechanical material tests as described in review papers [247, 248].

Cantilevers facilitate material characterization at small length scales. Materials show a different behaviour if scaled down and bulk property values are no longer valid. In 2003, Young's modulus of ultrathin single-crystalline silicon cantilevers was determined by means of the resonance method [249]. The beam thickness was varied from 300 nm down to 12 nm. At 12 nm, the cantilevers merely consist of 22 layers of silicon lattice in its thickness. That is, the length scale approaches the grain size of the structural material. A steady decrease in Young's modulus for thinner cantilevers was observed with a maximum decrease of 30% for the 12 nm thick beams compared with the 300 nm thick beams. At 300 nm, Young's modulus reaches the bulk value of 170 GPa. The studies concluded that for ultrathin single-crystalline silicon, surface effects play an important role in addition to bulk effects as the number of surface atoms is comparable to that in the bulk. The same size effect of Young's modulus has been reported for sub-100 nm chromium cantilevers determined by static deflection measurements [250].

In order to account for size dependent effects, Young's modulus $\widehat{E}$ is generally replaced by the effective Young's modulus $\widehat{E}_{\text{eff}}$. Gavan *et al* have determined the effective Young's modulus of silicon nitride cantilevers [251]. They observed a significant drop of the modulus for cantilevers thinner than 150 nm. By determining the modulus with the first two bending modes they could extract that the observed reduction in $\widehat{E}_{\text{eff}}$ is not caused by strain-independent surface stress or by a surface stress gradient in the silicon nitride film. Instead they related the size effect to the surface elasticity which is the strain-dependent part of the surface stress. The surface elasticity is taken into account by adding an infinitesimal thin surface layer to an Euler–Bernoulli beam. Therewith, the effective Young's modulus for a rectangular resonant cantilever beam can be written as [252, 253]

$$\widehat{E}_{\text{eff}} = \widehat{E} + 6\frac{C_{\text{s}}}{h}, \tag{5.1}$$

where h is the beam thickness and C_{s} is the surface elasticity. Gavan *et al* have successfully fitted this model to their data. The same model of E_{eff} has also been used by Sadeghian *et al* to describe Young's modulus reduction for silicon nanocantilevers [254]. Instead of using the resonance method, Sadeghian *et al* used the so-called pull-in instability to accurately study the effective Young's modulus. A schematic drawing and an SEM image of the cantilevers are shown in figure 23. A voltage is applied between the cantilevers and the substrate below and a camera observes at which bias the cantilever snaps to the surface. The snap-in voltage depends on the stiffness of the cantilever and can thus be used to calculate Young's modulus.

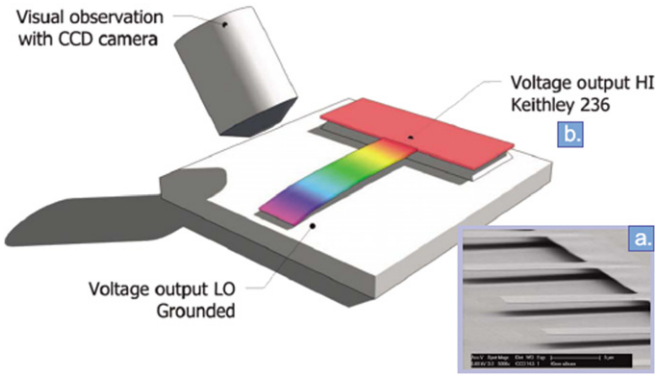

Figure 23. (*a*) SEM image of 40 nm thick silicon cantilevers (the scale bar is 5 μm). (*b*) Schematic view of the measurement set-up for the study of the size-dependent effective Young's modulus by means of the pull-in instability of the electrostatic cantilevers [254].

Cantilevers have also shown to be interesting for the characterization of polymer thin films. Nagy *et al* have been able to measure relaxation processes and to estimate Young's modulus of a phenyl substituted poly(p-phenylenevinylenes) (PVV) polymer spin-coated onto silicon cantilevers [255]. They have been able to observe changes of secondary transitions and Young's modulus during the conversion of the polymer by means of the resonance method.

Sangmin Jeon's group has measured changes in the resonant frequency and the deflection of silicon cantilevers coated with polymer films for varying temperatures [256, 257]. They have determined the mechanical properties in the vicinity of the glass transition. In particular, they have measured the temperature dependence of Young's modulus and the volume change of polystyrene and poly(vinyl acetate). Polystyrene films with varying thicknesses have been studied by Haramina *et al* [258]. They observed size effects for thin polystyrene layers with thicknesses below 100 nm. The glass transition temperature was lowered by about 10 K as the film thickness was decreased from 100 to 7.5 nm. The observed behaviour has been explained by modelling the polymer film as three layers (air/polymer interface, body, film/silicon interface), each with different properties.

Instead of coating a silicon cantilever with a polymer layer, all-polymer microcantilevers have been fabricated and characterized by the group of Hierold [38]. An SEM image of SU-8 cantilevers is shown in figure 24(*a*). By measuring the quality factor and the resonant frequencies of cured SU-8 cantilevers with different lengths at varying temperatures primary and secondary phase transition has been observed. Also, the temperature dependence of Young's modulus has been determined as shown in figure 24(*b*) [49]. Material ageing of the SU-8 cantilever has been observed by monitoring the resonant frequency of SU-8 cantilevers over more than 30 days as depicted in figure 24(*c*). Furthermore, water absorption mechanisms have been studied with the SU-8 cantilevers and a stiffening effect, so-called antiplasticization, has been observed for low relative humidifies followed by a plasticization at relative humidity levels above 15% [140].

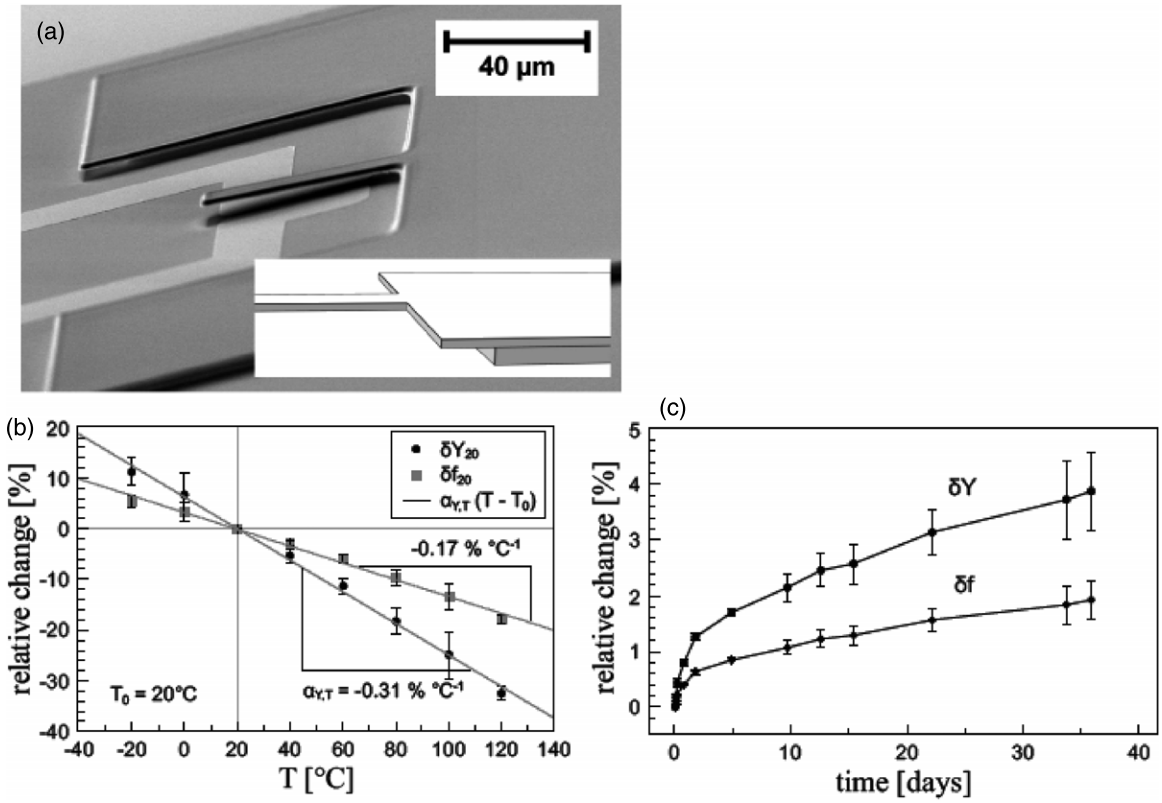

Figure 24. (*a*) SEM image of an SU-8 cantilever beam. (*b*) The average relative Young's modulus (here denoted Y) and resonant frequency change of 35 SU-8 cantilever microbeams with lengths from 13 to 180 μm with respect to the reference temperature $T_0 = 20\,^{\circ}$C. The measurements were performed at a pressure below 0.05 Pa. (*c*) The relative changes in Young's modulus and of the resonant frequency of nine SU-8 cantilevers with lengths from 30 to 140 mm, stored in a vacuum with a pressure $p < 0.01$ Pa. The temperature was sinusoidally cycled from -10 to 80 °C in a time interval of 60 min. The measurements were performed at a temperature of 20 °C [38].

5.7. Mass spectrometry

Mass spectrometry is used to determine the mass of molecules in many areas of biology and chemistry because it is fast and generally can determine the mass of molecules with good resolution. However, mass spectrometers actually measure mass-to-charge ratios, which means that the molecules have to be ionized in the first instance and, moreover, that the charge on the ionized molecules needs to be known before their mass can be extracted. These factors can cause problems because not all molecules are easy to ionize, and uncertainty about the charge of the molecules leads to uncertainty in the mass values reported.

Recently, Roukes *et al* have established an elegant technique based on nanometre-sized bridges where the true mass of molecules can, in principle, be determined without the need to ionize the molecules [224]. Moreover, the technique—called NEMS mass spectrometry—offers unrivalled mass sensitivity, which allows for real-time detection of individual molecular species. It also has the potential to work with extremely small sample volumes and to be miniaturized to make portable devices for identifying molecules.

First the mass sensing capability was tested by injecting gold nanoparticles with a diameter of 2.5 nm. As expected, the position of the added mass on the bridge influences the resulting frequency change: the change is largest at the centre of the bridge—where the amplitude of the oscillations is the largest—and zero at the ends. By comparing the distribution of measured frequency changes with the distribution expected for particles from a monodisperse source, it was possible to derive an average mass of the gold nanoparticles.

Next, mechanical mass spectrometry was performed on a solution of protein bovine albumin. From 578 binding events (resonant frequency jumps) it was possible to generate a spectrum showing that the sample consisted of monomers, dimers, trimers and pentamers and to calculate the ratio between them. These measurements demonstrate that it is possible to register the binding events of individual molecules.

6. Conclusion

The field of cantilever-based sensing is expanding both in terms of technology development and applications. More players are joining the field and more and more advanced devices are being developed. One of the challenges is the low probability of binding target molecules, because of the small sensor area. One solution is to implement large arrays of sensor. The millipede project at IBM [259], where thousands of cantilevers are used for data storage, has clearly demonstrated that it is possible to fabricate and control large cantilever arrays with integrated read-out. Recently, a collaboration between Caltech in USA and Leti in France [260] has been established in order to pursue the VLSI of nanomechanical sensors.

The surface chemistries developed and the applications reported have become more and more advanced in terms of detection limit and use of non-trivial probe-molecules. However, there are still several fundamental questions to be addressed. For example, the origin of surface stress changes is still not fully understood and several models have been presented on, for example, the generation of signals from DNA. Now researchers start to perform thorough and detailed studies on rather simple systems in order to fully understand the signal generations and, in parallel, model the surface stress generation.

The technology is in a maturing phase where some of the unanswered questions are now being addressed. One important experimental factor is the use of reference sensors for controlling the measurements and to reduce unspecific signals from for example changes in temperature. As the sensors are extremely sensitive to side effects such as change in temperature and measuring liquid there is a great risk of achieving false signals. It is therefore crucial to conduct measurements under very well controlled conditions and to perform control measurements by other supplementing techniques. Clearly, there is now a need for theoreticians, technology developers and application experts to initiate collaborative projects where critical aspects of cantilever and related sensing techniques are identified and carefully studied.

Also, change in surface stress, bulk stress and resonant frequency are coupled phenomena and there is a need for thorough studies on how these different mechanisms can be de-coupled. Before this is solved it will be difficult to obtain reliable and reproducible data. Since the cantilevers can give unique information on several parameters such as mass and surface stress changes, more information can be gained by measuring multiple parameters. The potential of cantilever sensors has not yet been fully explored.

In conclusion, the cantilever sensors have demonstrated unencumbered mass and surface stress sensitivity and it seems likely that these structures will be utilized in future products in, for example, diagnostics and drug discovery. The cantilever sensor field is exciting and dynamic. The limit for detection is constantly challenged and only the imagination sets the limit to new applications.

References

[1] Qavi A J, Washburn A L, Byeon J Y and Bailey R C 2009 Label-free technologies for quantitative multiparameter biological analysis *Anal. Bioanal. Chem.* **394** 121

[2] Fritz J 2008 Cantilever biosensors *Analyst* **133** 855

[3] Singamaneni S *et al* 2008 Bimaterial microcantilevers as a hybrid sensing platform *Adv. Mater.* **20** 653

[4] Waggoner P S and Craighead H G 2007 Micro- and nanomechanical sensors for environmental, chemical, and biological detection *Lab Chip* **7** 1238

[5] Carrascosa L G, Moreno M, Alvarez M and Lechuga L M 2006 Nanomechanical biosensors: a new sensing tool *Trac-Trends Anal. Chem.* **25** 196

[6] Boisen A and Thundat T 2009 Design & fabrication of cantilever array biosensors *Mater. Today* **12** 32

[7] Hwang K S, Lee S M, Kim S K, Lee J H and Kim T S 2009 Micro- and nanocantilever devices and systems for biomolecule detection *Annu. Rev. Anal. Chem.* **2** 77

[8] Binnig G, Quate C F and Gerber C 1986 Atomic force microscope *Phys. Rev. Lett.* **56** 930

[9] Albrecht T R, Akamine S, Carver T E and Quate C F 1990 Microfabrication of cantilever styli for the atomic force microscope *J. Vac. Sci. Technol.* A **8** 3386

[10] Wolter O, Bayer T and Greschner J 1991 Micromachined silicon sensors for scanning force microscopy *J. Vac. Sci. Technol.* B **9** 1353

[11] Thundat T, Warmack R J, Chen G Y and Allison D P 1994 Thermal and ambient-induced deflections of scanning force microscope cantilevers *Appl. Phys. Lett.* **64** 2894

[12] Thundat T, Wachter E A, Sharp S L and Warmack R J 1995 Detection of mercury-vapor using resonating microcantilevers *Appl. Phys. Lett.* **66** 1695

[13] Barnes J R, Stephenson R J, Woodburn C N, O'Shea S J, Welland M E, Rayment T, Gimzewski J K and Gerber C 1994 A femtojoule calorimeter using micromechanical sensors *Rev. Sci. Instrum.* **65** 3793

[14] Barnes J R, Stephenson R J, Welland M E, Gerber C and Gimzewski J K 1994 Photothermal spectroscopy with femtojoule sensitivity using a micromechanical device *Nature* **372** 79

[15] Raiteri R and Butt H-J 1995 Measuring electrochemically induced surface stress with an atomic force microscope *J. Phys. Chem.* **99** 15728

[16] Butt H J 1996 A sensitive method to measure changes in the surface stress of solids *J. Colloid Interface Sci.* **180** 251

[17] Berger R, Delamarche E, Lang H P, Gerber C, Gimzewski J K, Meyer E and Guntherodt H-J 1997 Surface stress in the self-assembly of alkanethiols on gold *Science* **276** 2021

[18] Lang H P *et al* 1998 A chemical sensor based on a micromechanical cantilever array for the identification of gases and vapors *Appl. Phys.* A **66** S61

[19] Fritz J, Baller M K, Lang H P, Rothuizen H, Vettiger P, Meyer E, Güntherodt H-J, Gerber C and Gimzewski J K 2000 Translating biomolecular recognition into nanomechanics *Science* **288** 316

[20] Boisen A, Thaysen J, Jensenius H and Hansen O 2000 Environmental sensors based on micromachined cantilevers with integrated read-out *Ultramicroscopy* **82** 11

[21] Lange D, Hagleitner C, Hierlemann A, Brand O and Baltes H 2002 Complementary metal oxide semiconductor cantilever arrays on a single chip: mass-sensitive detection of volatile organic compounds *Anal. Chem.* **74** 3084

[22] Wu G, Datar R H, Hansen K M, Thundat T, Cote R J and Majumdar A 2001 Bioassay of prostate-specific antigen (PSA) using microcantilevers *Nature Biotechnol.* **19** 856

[23] Ndieyira J W *et al* 2008 Nanomechanical detection of antibiotic mucopeptide binding in a model for superbug drug resistance *Nature Nanotechnol.* **3** 691

[24] Butt H J and Raiteri R 1999 Measurements of the surface tension and surface stress of solids *Surface Characterization Methods* (New York: Dekker)

[25] Berger R, Gerber C, Gimzewski J K, Meyer E and Guntherodt H J 1996 Thermal analysis using a micromechanical calorimeter *Appl. Phys. Lett.* **69** 40

[26] Feng X L, He R R, Yang P D and Roukes M L 2007 Very high frequency silicon nanowire electromechanical resonators *Nano Lett.* **7** 1953

[27] Ekinci K L, Huang X M H and Roukes M L 2004 Ultrasensitive nanoelectromechanical mass detection *Appl. Phys. Lett.* **84** 4469

[28] Yang Y T, Callegari C, Feng X L, Ekinci K L and Roukes M L 2006 Zeptogram-scale nanomechanical mass sensing *Nano Lett.* **6** 583

[29] Ekinci K L, Yang Y T and Roukes M L 2004 Ultimate limits to inertial mass sensing based upon nanoelectromechanical systems *J. Appl. Phys.* **95** 2682

[30] Rodahl M, Hook F, Krozer A, Brzezinski P and Kasemo B 1995 Quartz-crystal microbalance setup for frequency and Q-factor measurements in gaseous and liquid environments *Rev. Sci. Instrum.* **66** 3924

[31] Cagliani A and Davis Z J 2009 Bulk disk resonator based ultrasensitive mass sensor *IEEE Sensors 2009 (Christchurch, New Zealand)* vols 1–3 (New York: IEEE) 1254pp

[32] Lavrik N V and Datskos P G 2003 Femtogram mass detection using photothermally actuated nanomechanical resonators *Appl. Phys. Lett.* **82** 2697

[33] Li M, Tang H X and Roukes M L 2007 Ultra-sensitive NEMS-based cantilevers for sensing, scanned probe and very high-frequency applications *Nature Nanotechnol.* **2** 114

[34] Young W C, Budynas R G and Roark R J 2002 *Roark's Formulas for Stress and Strain* (Boston, MA: McGraw-Hill)

[35] Cleland A N 2003 *Foundations of Nanomechanics* (Berlin: Springer)

[36] Timoshenko S and Woinowski-Krieger S 1970 *Theory of Plates and Shells* (New York: McGraw-Hill)

[37] Weaver W, Timoshenko S P and Young D H 1990 *Vibration Problems in Engineering* (New York: Wiley)

[38] Schmid S 2009 *Electrostatically Actuated All-Polymer Microbeam Resonators—Characterization and Application* ed C Hierold (Toenning: Der Andere)

[39] Dohn S, Sandberg R, Svendsen W and Boisen A 2005 Enhanced functionality of cantilever based mass sensors using higher modes *Appl. Phys. Lett.* **86** 233501

[40] Yasumura K Y, Stowe T D, Chow E M, Pfafman T, Kenny T W, Stipe B C and Rugar D 2000 Quality factors in micron- and submicron-thick cantilevers *J. Microelectromech. Syst.* **9** 117

[41] Lifshitz R and Roukes M L 2000 Thermoelastic damping in micro- and nanomechanical systems *Phys. Rev.* B **61** 5600

[42] Mohanty P, Harrington D A, Ekinci K L, Yang Y T, Murphy M J and Roukes M L 2002 Intrinsic dissipation in high-frequency micromechanical resonators *Phys. Rev.* B **66** 085416

[43] Stemme G 1991 Resonant silicon sensors *J. Micromech. Microeng.* **1** 113

[44] Photiadis D M and Judge J A 2004 Attachment losses of high Q oscillators *Appl. Phys. Lett.* **85** 482

[45] Blom F R, Bouwstra S, Elwenspoek M and Fluitman J H J 1992 Dependence of the quality factor of micromachined silicon beam resonators on pressure and geometry *J. Vac. Sci. Technol.* B **10** 19

[46] Sandberg R, Molhave K, Boisen A and Svendsen W 2005 Effect of gold coating on the Q-factor of a resonant cantilever *J. Micromech. Microeng.* **15** 2249

[47] Calleja M, Nordstrom M, Alvarez M, Tamayo J, Lechuga L M and Boisen A 2005 Highly sensitive polymer-based cantilever-sensors for DNA detection *Ultramicroscopy* **105** 215

[48] Verbridge S S, Parpia J M, Reichenbach R B, Bellan L M and Craighead H G 2006 High quality factor resonance at room temperature with nanostrings under high tensile stress *J. Appl. Phys.* **99** 124304

[49] Schmid S and Hierold C 2008 Damping mechanisms of single-clamped and prestressed double-clamped resonant polymer microbeams *J. Appl. Phys.* **104** 093516

[50] Verbridge S S, Shapiro D F, Craighead H G and Parpia J M 2007 Macroscopic tuning of nanomechanics: substrate bending for reversible control of frequency and quality factor of nanostring resonators *Nano Lett.* **7** 1728

[51] Schmid S, Malm B and Boisen A 2011 Quality factor improvement of silicon nitride micro string resonators *24th Int. Conf. on Micro Electro Mechanical Systems (IEEE MEMS) (Cancun, Mexico)*

[52] Putman C A J, Degrooth B G, Vanhulst N F and Greve J 1992 A detailed analysis of the optical beam deflection technique for use in atomic force microscopy *J. Appl. Phys.* **72** 6

[53] Beck R G, Eriksson M A, Topinka M A, Westervelt R M, Maranowski K D and Gossard A C 1998 GaAs/AlGaAs self-sensing cantilevers for low temperature scanning probe microscopy *Appl. Phys. Lett.* **73** 1149

[54] Cleland A N and Roukes M L 1999 External control of dissipation in a nanometer-scale radiofrequency mechanical resonator *Sensors Actuators* A **72** 256

[55] Jensenius H, Thaysen J, Rasmussen A A, Veje L H, Hansen O and Boisen A 2000 A microcantilever-based alcohol vapor sensor-application and response model *Appl. Phys. Lett.* **76** 2615

[56] Zhang Y and Blencowe M P 2002 Intrinsic noise of a micromechanical displacement detector based on the radio-frequency single-electron transistor *J. Appl. Phys.* **91** 4249

[57] Ghatnekar-Nilsson S, Forsen E, Abadal G, Verd J, Campabadal F, Perez-Murano F, Esteve J, Barniol N, Boisen A and Montelius L 2005 Resonators with integrated CMOS circuitry for mass sensing applications, fabricated by electron beam lithography *Nanotechnology* **16** 98

[58] Lee D, Kim S, Jung N, Thundat T and Jeon S 2009 Effects of gold patterning on the bending profile and frequency response of a microcantilever *J. Appl. Phys.* **106** 024310

[59] Dohn S, Svendsen W, Boisen A and Hansen O 2007 Mass and position determination of attached particles on cantilever based mass sensors *Rev. Sci. Instrum.* **78** 103303

[60] Senturia S D 2002 *Energy Methods, Microsystem Design* (Dordrecht: Kluwer) 239pp

[61] Dohn S, Schmid S, Amiot F and Boisen A 2010 Position and mass determination of multiple particles using cantilever based mass sensors *Appl. Phys. Lett.* **97** 044103

[62] Schmid S, Dohn S and Boisen A 2010 Real-time particle mass spectrometry based on resonant micro strings *Sensors* **10** 8092

[63] Stoney G G 1909 The tension of metallic films deposited by electrolysis *Proc. R. Soc. Lond.* A **82** 172

[64] Jaccodin Rj and Schlegel W A 1966 Measurement of strains at Si–SiO_2 interface *J. Appl. Phys.* **37** 2429

[65] Godin M, Tabard-Cossa V, Grutter P and Williams P 2001 Quantitative surface stress measurements using a microcantilever *Appl. Phys. Lett.* **79** 551

[66] Zang J and Liu F 2007 Theory of bending of Si nanocantilevers induced by molecular adsorption: a modified Stoney formula for the calibration of nanomechanochemical sensors *Nanotechnology* **18** 405501

[67] Hagan M F, Majumdar A and Chakraborty A K 2002 Nanomechanical forces generated by surface grafted DNA *J. Phys. Chem.* B **106** 10163

[68] Liu F, Zhang Y and Ou-Yang Z C 2003 Flexoelectric origin of nanomechanic deflection in DNA-microcantilever system *Biosensors Bioelectron.* **18** 655

[69] Begley M R, Utz M and Komaragiri U 2005 Chemo-mechanical interactions between adsorbed molecules and thin elastic films *J. Mech. Phys. Solids* **53** 2119

[70] Wu G, Ji H, Hansen K, Thundat T, Datar R, Cote R, Hagan M F, Chakraborty A K and Majumdar A 2001 Origin of nanomechanical cantilever motion generated from biomolecular interactions *Proc. Natl Acad. Sci. USA* **98** 1560

[71] McKendry R *et al* 2002 Multiple label-free biodetection and quantitative dna-binding assays on a nanomechanical cantilever array *Proc. Natl Acad. Sci. USA* **99** 9783
[72] Watari M, Galbraith J, Lang H P, Sousa M, Hegner M, Gerber C, Horton M A and McKendry R A 2007 Investigating the molecular mechanisms of in-plane mechanochemistry on cantilever arrays *J. Am. Chem. Soc.* **129** 601
[73] Sushko M L, Harding J H, Shluger A L, McKendry R A and Watari M 2008 Physics of nanomechanical biosensing on cantilever arrays *Adv. Mater.* **20** 3848
[74] Godin M, Tabard-Cossa V, Miyahara Y, Monga T, Williams P J, Beaulieu L Y, Lennox R B and Grutter P 2010 Cantilever-based sensing: the origin of surface stress and optimization strategies *Nanotechnology* **21** 075501
[75] Hansen A G, Mortensen M W, Andersen J E T, Ulstrup J, Kühle A, Garnæs J and Boisen A 2001 Stress formation during self-assembly of alkanethiols *Probe Microsc.* **2** 139
[76] Godin M, Williams P J, Tabard-Cossa V, Laroche O, Beaulieu L Y, Lennox R B and Grutter P 2004 Surface stress, kinetics, and structure of alkanethiol self-assembled monolayers *Langmuir* **20** 7090
[77] Mertens J, Calleja M, Ramos D, Taryn A and Tamayo J 2007 Role of the gold film nanostructure on the nanomechanical response of microcantilever sensors *J. Appl. Phys.* **101** 034904
[78] Arroyo-Hernandez M, Tamayo J and Costa-Kramer J L 2009 Stress and DNA assembly differences on cantilevers gold coated by resistive and e-beam evaporation techniques *Langmuir* **25** 10633
[79] Mertens J, Rogero C, Calleja M, Ramos D, Martin-Gago J A, Briones C and Tamayo J 2008 Label-free detection of DNA hybridization based on hydration-induced tension in nucleic acid films *Nature Nanotechnol.* **3** 301
[80] Shu W M, Liu D S, Watari M, Riener C K, Strunz T, Welland M E, Balasubramanian S and McKendry R A 2005 DNA molecular motor driven micromechanical cantilever arrays *J. Am. Chem. Soc.* **127** 17054
[81] Timoshenko S 1925 Analysis of bi-metal thermostats *J. Opt. Soc. Am.* **11** 233
[82] Zhiyu H, Thundat T and Warmack R J 2001 Investigation of adsorption and absorption-induced stresses using microcantilever sensors *J. Appl. Phys.* **90** 427
[83] Lavrik N V, Sepaniak M J and Datskos P G 2004 Cantilever transducers as a platform for chemical and biological sensors *Rev. Sci. Instrum.* **75** 2229
[84] LeMieux M C, McConney M E, Lin Y-H, Singamaneni S, Jiang H, Bunning T J and Tsukruk V V 2006 Polymeric nanolayers as actuators for ultrasensitive thermal bimorphs *Nano Lett.* **6** 730
[85] He J-H *et al* 2009 A thermal sensor and switch based on a plasma polymer/ZnO suspended nanobelt bimorph structure *Nanotechnology* **20** 065502
[86] Gimzewski J K, Gerber C, Meyer E and Schlittler R R 1994 Observation of a chemical reaction using a micromechanical sensor *Chem. Phys. Lett.* **217** 589
[87] Singamaneni S, McConney M E, LeMieux M C, Jiang H, Enlow J O, Bunning T J, Naik R R and Tsukruk V V 2007 Polymer-silicon flexible structures for fast chemical vapor detection *Adv. Mater.* **19** 4248
[88] Schmid S, Wägli P and Hierold C 2008 All-polymer microstring resonant humidity sensor with enhanced sensitivity due to change of intrinsic stress *EUROSENSORS 22nd Conf. (Dresden, Germany)* p 697
[89] Pandey A K, Gottlieb O, Shtempluck O and Buks E 2010 Performance of an AuPd micromechanical resonator as a temperature sensor *Appl. Phys. Lett.* **96** 203105
[90] www.concentris.ch
[91] www.micromotive.de
[92] Yang J, Ono T and Esashi M 2000 Mechanical behavior of ultrathin microcantilever *Sensors Actuators* A **82** 102
[93] Ramos D, Arroyo-Hernandez M, Gil-Santos E, Tong H D, Van Rijn C, Calleja M and Tamayo J 2009 Arrays of dual nanomechanical resonators for selective biological detection *Anal. Chem.* **81** 2274
[94] Kovacs G T A, Maluf N I and Petersen K E 1998 Bulk micromachining of silicon *Proc. IEEE* **86** 1536
[95] http://www.svmi.com
[96] http://www.soitec.com/en/index.php
[97] http://www.universitywafers.com
[98] May G S and Sze S M 2004 *Photolithography, Fundamentals of Semiconductor Fabrication* (New York: Wiley)
[99] McCord M A and Rooks M J 1997 Electron beam lithography *Handbook of Microlithography, Micromachining, and Microfabrication* vol 1 ed P Rai-Choudhury (Washington, DC: SPIE)
[100] Garrou P, Bower C and Ramm P 2008 *Handbook of 3D Integration* (Weinheim: Wiley)
[101] Bagolini A, Pakula L, Scholtes T L M, Pham H T M, French P J and Sarro P M 2002 Polyimide sacrificial layer and novel materials for post-processing surface micromachining *J. Micromech. Microeng.* **12** 385
[102] Geim A K and Novoselov K S 2007 The rise of graphene *Nature Mater.* **6** 183
[103] Robertson J 2002 Diamond-like amorphous carbon *Mater. Sci. Eng.* R **37** 129
[104] Pechmann R, Kohler J M, Fritzsche W, Schaper A and Jovin T M 1994 The Novolever: a new cantilever for scanning force microscopy microfabricated from polymeric materials *Rev. Sci. Instrum.* **65** 3702
[105] Genolet G, Brugger J, Despont M, Drechsler U, Vettiger P, de Rooij N F and Anselmetti D 1999 Soft, entirely photoplastic probes for scanning force microscopy *Rev. Sci. Instrum.* **70** 2398
[106] Hopcroft M, Kramer T, Kim G, Takashima K, Higo Y, Moore D and Brugger J 2005 Micromechanical testing of SU-8 cantilevers *Fatigue Fract. Eng. Mater. Struct.* **28** 735
[107] Calleja M, Tamayo J, Johansson A, Rasmussen P, Lechuga L M and Boisen A 2003 Polymeric cantilever arrays for biosensing applications *Sensor Lett.* **1** 20
[108] Ransley J H T, Watari M, Sukumaran D, McKendry R A and Seshia A A 2006 SU8 bio-chemical sensor microarrays *Microelectron. Eng.* **83** 1621
[109] Wang X, Ryu K S, Bullen D A, Zou J, Zhang H, Mirkin C A and Liu C 2003 Scanning probe contact printing *Langmuir* **19** 8951
[110] Gaitas A and Gianchandani Y B 2006 An experimental study of the contact mode AFM scanning capability of polyimide cantilever probes *Ultramicroscopy* **106** 874
[111] McFarland A W, Poggi M A, Bottomley L A and Colton J S 2004 Production and characterization of polymer microcantilevers *Rev. Sci. Instrum.* **75** 2756
[112] McFarland A W, Poggi M A, Bottomley L A and Colton J S 2004 Injection moulding of high aspect ratio micron-scale thickness polymeric microcantilevers *Nanotechnology* **15** 1628
[113] McFarland A W and Colton J S 2005 Chemical sensing with micromolded plastic microcantilevers *J. Microelectromech. Syst.* **14** 1375
[114] Zhang X R and Xu X 2004 Development of a biosensor based on laser-fabricated polymer microcantilevers *Appl. Phys. Lett.* **85** 2423
[115] Lee L P, Berger S A, Liepmann D and Pruitt L 1998 High aspect ratio polymer microstructures and cantilevers for bioMEMS using low energy ion beam and photolithography *Sensors Actuators* A **71** 144

[116] Yao T-J, Yang X and Tai Y-C 2002 BrF3 dry release technology for large freestanding parylene microstructures and electrostatic actuators *Sensors Actuators* A **97/98** 771
[117] Katragadda R, Wang Z, Khalid W, Li Y and Xu Y 2007 Parylene cantilevers integrated with polycrystalline silicon piezoresistors for surface stress sensing *Appl. Phys. Lett.* **91** 083505
[118] Greve A, Keller S, Vig A L, Kristensen A, Larsson D, Yvind K, Hvam J M, Cerruti M, Majumdar A and Boisen A 2010 Thermoplastic microcantilevers fabricated by nanoimprint lithography *J. Micromech. Microeng.* **20** 015009
[119] www.topas.com
[120] Zou J, Wang X, Bullen D, Ryu K, Liu C and Mirkin C A 2004 A mould-and-transfer technology for fabricating scanning probe microscopy probes *J. Micromech. Microeng.* **14** 204
[121] Kramer P, Sharma A K, Hennecke E E and Yasuda H 1984 Polymerization of para-xylylene derivatives (parylene polymerization): I. Deposition kinetics for parylene N and parylene C *J. Polym. Sci.: Polym. Chem. Edn* **22** 475
[122] Ibbotson R H, Dunn R J, Djakov V, Ferrigno P K and Huq S E 2008 Polyimide microcantilever surface stress sensor using low-cost, rapidly-interchangeable, spring-loaded microprobe connections *Microelectron. Eng.* **85** 1314
[123] Guo L J 2004 Recent progress in nanoimprint technology and its applications *J. Phys. D: Appl. Phys.* **37** R123
[124] Schift H 2008 Nanoimprint lithography: an old story in modern times? A review *J. Vac. Sci. Technol.* B **26** 458
[125] Johansson A, Blagoi G and Boisen A 2006 Polymeric cantilever-based biosensors with integrated readout *Appl. Phys. Lett.* **89** 173505
[126] Genolet G 2001 New photoplastic fabrication techniques and devices based on high aspect ratio photoresist *PhD Thesis* Ecole Polytechnique Fédérale de Lausanne
[127] Dellmann L, Roth S, Beuret C, Racine G A, Lorenz H, Despont M, Renaud P, Vettiger P and de Rooij N F 1998 Fabrication process of high aspect ratio elastic and SU-8 structures for piezoelectric motor applications *Sensors Actuators* A **70** 42
[128] Schmid S, Wendlandt M, Junker D and Hierold C 2006 Nonconductive polymer microresonators actuated by the Kelvin polarization force *Appl. Phys. Lett.* **89** 163506
[129] Jeppesen C 2008 Optically actuated cantilevers *Masters Thesis* Technical University of Denmark, Lyngby
[130] Martin C, Llobera A, Villanueva G, Voigt A, Gruetzner G, Brugger J and Perez-Murano F 2009 Stress and aging minimization in photoplastic AFM probes *Microelectron. Eng.* **86** 1226
[131] Mouaziz S, Boero G, Popovic R S and Brugger J A B J 2006 Polymer-based cantilevers with integrated electrodes *J. microelectromech. Syst.* **15** 890
[132] Foulds I G, Johnstone R W and Parameswaran M 2008 Polydimethylglutarimide (PMGI) as a sacrificial material for SU-8 surface-micromachining *J. Micromech. Microeng.* **18** 075011
[133] Legtenberg R, Tilmans H A C, Elders J and Elwenspoek M 1994 Stiction of surface micromachined structures after rinsing and drying: model and investigation of adhesion mechanisms *Sensors Actuators* A **43** 230
[134] Cheng M C, Gadre A P, Garra J A, Nijdam A J, Luo C, Schneider T W, White R C, Currie J F and Paranjape M 2004 Dry release of polymer structures with anti-sticking layer *J. Vac. Sci. Technol.* A **22** 837
[135] Haefliger D, Nordstrom M, Rasmussen P A and Boisen A 2005 Dry release of all-polymer structures *Microelectron. Eng.* **78/79** 88
[136] Keller S, Haefliger D and Boisen A 2007 Optimized plasma-deposited fluorocarbon coating for dry release and passivation of thin SU-8 cantilevers *J. Vac. Sci. Technol.* B **25** 1903
[137] Manias E, Chen J, Fang N and Zhang X 2001 Polymeric micromechanical components with tunable stiffness *Appl. Phys. Lett.* **79** 1700
[138] Bayindir Z, Sun Y, Naughton M J, LaFratta C N, Baldacchini T, Fourkas J T, Stewart J, Saleh B E A and Teich M C 2005 Polymer microcantilevers fabricated via multiphoton absorption polymerization *Appl. Phys. Lett.* **86** 064105
[139] Tenje M, Keller S, Dohn S, Davis Z J and Boisen A 2010 Drift study of SU8 cantilevers in liquid and gaseous environments *Ultramicroscopy* **101** 596
[140] Schmid S, Kühne S and Hierold C 2009 Influence of air humidity on polymeric microresonators *J. Micromech. Microeng.* **19** 065018
[141] Keller S, Haefliger D and Boisen A 2010 Fabrication of thin SU-8 cantilevers: initial bending, release and time-stability *J. Micromech. Microeng.* **20** 045024
[142] Haefliger D, Hansen O and Boisen A 2006 Self-positioning of polymer membranes driven by thermomechanically induced plastic deformation *Adv. Mater.* **18** 238
[143] Blagoi G, Keller S, Persson F, Boisen A and Jakobsen M H 2008 Photochemical modification and patterning of SU-8 using anthraquinone photolinkers *Langmuir* **24** 9929
[144] Tao S L, Popat K C, Norman J J and Desai T A 2008 Surface modification of SU-8 for enhanced biofunctionality and nonfouling properties *Langmuir* **24** 2631
[145] Fischer L M, Pedersen C, Elkjær K, Noeth N N, Dohn S, Boisen A and Tenje M 2011 Development of a microfabricated electrochemical-cantilever hybrid platform *Sensors Actuators* B accepted
[146] Ivanov T, Gotszalk T, Grabiec P, Tomerov E and Rangelow I W 2003 Thermally driven micromechanical beam with piezoresistive deflection readout *Microelectron. Eng.* **67/68** 550
[147] Rasmussen P A, Thaysen J, Hansen O, Eriksen S C and Boisen A 2003 Optimised cantilever biosensor with piezoresistive read-out *Ultramicroscopy* **97** 371
[148] Yu X M, Thaysen J, Hansen O and Boisen A 2002 Optimization of sensitivity and noise in piezoresistive cantilevers *J. Appl. Phys.* **92** 6296
[149] Thaysen J, Marie R and Boisen A 2001 Cantilever-based bio-chemical sensor integrated in a microliquid handling system *14th IEEE Int. Conf. on Micro Electro Mechanical Systems, Technical Digest (Interlaken, Switzerland)* 401pp
[150] Thaysen J, Yalcinkaya A D, Vettiger P and Menon A 2002 Polymer-based stress sensor with integrated readout *J. Phys. D: Appl. Phys.* **35** 2698
[151] Johansson A, Calleja M, Rasmussen P A and Boisen A 2005 SU-8 cantilever sensor system with integrated readout *Sensors Actuators* A **123/124** 111
[152] Johansson A 2006 SU-8 cantilever sensor with integrated readout *PhD Thesis* Technical University of Denmark, Lyngby
[153] Jiguet S, Bertsch A, Hofmann H and Renaud P 2004 SU8-silver photosensitive nanocomposite *Adv. Eng. Mater.* **6** 719
[154] Lillemose M, Gammelgaard L, Richter J, Thomsen E V and Boisen A 2008 Epoxy based photoresist/carbon nanoparticle composites *Compos. Sci. Technol.* **68** 1831
[155] Damean N, Parviz B A, Lee J N, Odom T and Whitesides G M 2005 Composite ferromagnetic photoresist for the fabrication of microelectromechanical systems *J. Micromech. Microeng.* **15** 29
[156] Fakhfouri V, Ingrosso C, Curri M L, Striccoli M, Agostiano A, Voigt A, Gruetzner G and Brugger J 2009 An epoxy photoresist modified by luminescent

nanocrystals for the fabrication of 3D high-aspect-ratio microstructures *Adv. Func. Mat.* **17** 2009–17
[157] Gammelgaard L, Rasmussen P A, Calleja M, Vettiger P and Boisen A 2006 Microfabricated photoplastic cantilever with integrated photoplastic/carbon based piezoresistive strain sensor *Appl. Phys. Lett.* **88** 113508
[158] Lillemose M, Spieser M, Christiansen N O, Christensen A and Boisen A 2008 Intrinsically conductive polymer thin film piezoresistors *Microelectron. Eng.* **85** 969
[159] Mateiu R, Lillemose M, Hansen T S, Boisen A and Geschke O 2007 Reliability of poly 3,4-ethylenedioxythiophene strain gauge *Microelectron. Eng.* **84** 1270
[160] Seena V, Rajorya A, Pant P, Mukherji S and Rao V R 2009 Polymer microcantilever biochemical sensors with integrated polymer composites for electrical detection *Solid State Sci.* **11** 1606
[161] Ji H-F, Hansen K M, Hu Z and Thundat T 2001 Detection of pH variation using modified microcantilever sensors *Sensors Actuators* B **72** 233
[162] Lang H P, Baller M K, Berger R, Gerber C, Gimzewski J K, Battiston F M, Fornaro P, Ramseyer J P, Meyer E and Guntherodt H J 1999 An artificial nose based on a micromechanical cantilever array *Anal. Chim. Acta* **393** 59
[163] Lang H P *et al* 1998 Sequential position readout from arrays of micromechanical cantilever sensors *Appl. Phys. Lett.* **72** 383
[164] Lim S H, Raorane D, Satyanarayana S and Majumdar A 2006 Nano-chemo-mechanical sensor array platform for high-throughput chemical analysis *Sensors Actuators* B **119** 466
[165] Yue M, Stachowiak J C, Lin H, Datar R, Cote R and Majumdar A 2008 Label-free protein recognition two-dimensional array using nanomechanical sensors *Nano Lett.* **8** 520
[166] Yue M, Lin H, Dedrick D E, Satyanarayana S, Majumdar A, Bedekar A S, Jenkins J W and Sundaram S 2004 A 2-D microcantilever array for multiplexed biomolecular analysis *J. Microelectromech. Syst.* **13** 290
[167] Mertens J, Alvarez M and Tamayo J 2005 Real-time profile of microcantilevers for sensing applications *Appl. Phys. Lett.* **87** 234102
[168] Amiot F and Roger J P 2006 Nomarski imaging interferometry to measure the displacement field of micro-electro-mechanical systems *Appl. Opt.* **45** 7800
[169] Amiot F, Hild F, Kanoufi F and Roger J P 2007 Identification of the electroelastic coupling from full multi-physical fields measured at the micrometre scale *J. Phys. D: Appl. Phys.* **40** 3314
[170] Larsson D, Greve A, Hvam J M, Boisen A and Yvind K 2009 Self-mixing interferometry in vertical-cavity surface-emitting lasers for nanomechanical cantilever sensing *Appl. Phys. Lett.* **94** 091103
[171] Zinoviev K, Dominguez C, Plaza J A, Busto V J C and Lechuga L M 2006 A novel optical waveguide microcantilever sensor for the detection of nanomechanical forces *J. Lightwave Technol.* **24** 2132
[172] Nordström M, Zauner D A, Calleja M, Hubner J and Boisen A 2007 Integrated optical readout for miniaturization of cantilever-based sensor system *Appl. Phys. Lett.* **91** 103512
[173] Noh J W, Anderson R, Kim S, Cardenas J and Nordin G P 2008 In-plane photonic transduction of silicon-on-insulator microcantilevers *Opt. Express* **16** 12114
[174] Nordström M 2007 Integrated optical read-out for polymeric cantilever-based sensors *PhD Thesis* DTU, Lyngby
[175] Blanc N, Brugger J, de Rooij N F and Durig U 1996 Scanning force microscopy in the dynamic mode using microfabricated capacitive sensors *J. Vac. Sci. Technol.* B **14** 901
[176] Bay J, Bouwstra S, Laegsgaard E and Hansen O 1995 Micromachined AFM transducer with differential capacitive read-out *J. Micromech. Microeng.* **5** 161
[177] Kim S J, Ono T and Esashi M 2006 Capacitive resonant mass sensor with frequency demodulation detection based on resonant circuit *Appl. Phys. Lett.* **88** 053116
[178] Villarroya M *et al* 2006 System on chip mass sensor based on polysilicon cantilevers arrays for multiple detection *Sensors Actuators* A **132** 154
[179] Forsen E *et al* 2005 Ultrasensitive mass sensor fully integrated with complementary metal-oxide-semiconductor circuitry *Appl. Phys. Lett.* **87** 043507
[180] Verd J *et al* 2005 Design, fabrication, and characterization of a submicroelectromechanical resonator with monolithically integrated CMOS readout circuit *J. Microelectromech. Syst.* **14** 508
[181] Forsen E *et al* 2004 Fabrication of cantilever based mass sensors integrated with CMOS using direct write laser lithography on resist *Nanotechnology* **15** S628
[182] Teva J, Abadal G, Torres F, Verd J, Perez-Murano F and Barniol N 2006 A femtogram resolution mass sensor platform, based on SOI electrostatically driven resonant cantilever: I. Electromechanical model and parameter extraction *Ultramicroscopy* **106** 800
[183] Arcamone J, Rius G, Abadal G, Teva J, Barniol N and Perez-Murano F 2006 Micro/nanomechanical resonators for distributed mass sensing with capacitive detection *Microelectron. Eng.* **83** 1216
[184] Ghatnekar-Nilsson S, Karlsson I, Kvennefors A, Luo G, Zela V, Arlelid M, Parker T, Montelius L and Litwin A 2009 A new multifunctional platform based on high aspect ratio interdigitated NEMS structures *Nanotechnology* **20** 175502
[185] Itoh T and Suga T 1993 Development of a force sensor for atomic force microscopy using piezoelectric thin films *Nanotechnology* **4** 218
[186] Itoh T and Suga T 1994 Piezoelectric force sensor for scanning force microscopy *Sensors Actuators* A **43** 305
[187] Lee C, Itoh T and Suga T 1999 Self-excited piezoelectric PZT microcantilevers for dynamic SFM—with inherent sensing and actuating capabilities *Sensors Actuators* A **72** 179
[188] Minne S C, Manalis S R, Atalar A and Quate C F 1996 Contact imaging in the atomic force microscope using a higher order flexural mode combined with a new sensor *Appl. Phys. Lett.* **68** 1427
[189] Watanabe S and Fujii T 1996 Micro-fabricated piezoelectric cantilever for atomic force microscopy *Rev. Sci. Instrum.* **67** 3898
[190] Adams J D, Rogers B, Manning L, Hu Z, Thundat T, Cavazos H and Minne S C 2005 Piezoelectric self-sensing of adsorption-induced microcantilever bending *Sensors Actuators* A **121** 457
[191] Xu S and Mutharasan R 2010 Rapid and sensitive detection of Giardia lamblia using a piezoelectric cantilever biosensor in finished and source waters *Environ. Sci. Technol.* **44** 1736
[192] Lee J H, Hwang K S, Park J, Yoon K H, Yoon D S and Kim T S 2005 Immunoassay of prostate-specific antigen (PSA) using resonant frequency shift of piezoelectric nanomechanical microcantilever *Biosensors Bioelectron.* **20** 2157
[193] Cha B H, Lee S M, Park J C, Hwang K S, Kim S K, Lee Y S, Ju B K and Kim T S 2009 Detection of Hepatitis B Virus (HBV) DNA at femtomolar concentrations using a silica nanoparticle-enhanced microcantilever sensor *Biosensors Bioelectron.* **25** 130

[194] http://www.microsystem.re.kr
[195] Cleland A N, Pophristic M and Ferguson I 2001 Single-crystal aluminum nitride nanomechanical resonators *Appl. Phys. Lett.* **79** 2070
[196] Cleland A N and Roukes M L 1996 Fabrication of high frequency nanometer scale mechanical resonators from bulk Si crystals *Appl. Phys. Lett.* **69** 2653
[197] Tortonese M, Barrett R C and Quate C F 1993 Atomic resolution with an atomic force microscope using piezoresistive detection *Appl. Phys. Lett.* **62** 834
[198] Linnemann R, Gotszalk T, hadjiski L and Rangelow I W 1995 Characterization of a cantilever with an integrated deflection sensor *Thin Solid Films* **264** 159
[199] http://www.sii.co.jp/info/eg/mems2.html
[200] Park J H, Graf D, Murphy T P, Schmiedeshoff G M and Tozer S W 2009 High resolution miniature dilatometer based on an atomic force microscope piezocantilever *Rev. Sci. Instrum.* **80** 116101
[201] Kim S, Rahman T, Senesac L R, Davison B H and Thundat T 2009 Piezoresistive cantilever array sensor for consolidated bioprocess monitoring *Scanning* **31** 204
[202] Baker G A, Desikan R and Thundat T 2008 Label-free sugar detection using phenylboronic acid-functionalized piezoresistive microcantilevers *Anal. Chem.* **80** 4860
[203] Yoshikawa G, Lang H P, Akiyama T, Aeschimann L, Staufer U, Vettiger P, Aono M, Sakurai T and Gerber C 2009 Sub-ppm detection of vapors using piezoresistive microcantilever array sensors *Nanotechnology* **20** 015501
[204] Thaysen J, Boisen A, Hansen O and Bouwstra S 2000 Atomic force microscopy probe with piezoresistive read-out and a highly symmetrical Wheatstone bridge arrangement *Sensors Actuators* A **83** 47
[205] Rasmussen P A, Thaysen J, Bouwstra S and Boisen A 2001 Modular design of AFM probe with sputtered silicon tip *Sensors Actuators* A **92** 96
[206] Yu H T, Li X X, Gan X H, Liu Y J, Liu X, Xu P C, Li J G and Liu M 2009 Resonant-cantilever bio/chemical sensors with an integrated heater for both resonance exciting optimization and sensing repeatability enhancement *J. Micromechan. Microeng.* **19** 045023
[207] Narducci M, Figueras E, Lopez M J, Gracia I, Santander J, Ivanov P, Fonseca L and Cane C 2009 Sensitivity improvement of a microcantilever based mass sensor *Microelectron. Eng.* **86** 1187
[208] Park S J, Doll J C and Pruitt B L 2010 Piezoresistive cantilever performance: I. Analytical model for sensitivity *J. Microelectromech. Syst.* **19** 137
[209] Park S J, Doll J C, Rastegar A J and Pruitt B L 2010 Piezoresistive cantilever performance: II. Optimization *J. Microelectromech. Syst.* **19** 149
[210] Hierlemann A, Lange D, Hagleitner C, Kerness N, Koll A, Brand O and Baltes H 2000 Application-specific sensor systems based on CMOS chemical microsensors *Sensors Actuators* B **70** 2
[211] Voiculescu I, Zaghloul M E, McGill R A, Houser E J and Fedder G K 2005 Electrostatically actuated resonant microcantilever beam in CMOS technology for the detection of chemical weapons *IEEE Sensors J.* **5** 641
[212] Kenny T W, Waltman S B, Reynolds J K and Kaiser W J 1991 Micromachined silicon tunnel sensor for motion detection *Appl. Phys. Lett.* **58** 100
[213] Scheible D V, Erbe A and Blick R H 2002 Tunable coupled nanomechanical resonators for single-electron transport *New J. Phys.* **4** 86
[214] Scheible D V, Erbe A and Blick R H 2003 Dynamic control and modal analysis of coupled nano-mechanical resonators *Appl. Phys. Lett.* **82** 3333
[215] Dohn S, Hansen O and Boisen A 2006 Cantilever based mass sensor with hard contact readout *Appl. Phys. Lett.* **88** 264104
[216] Dohn S, Hansen O and Boisen A 2008 Measurement of the resonant frequency of nano-scale cantilevers by hard contact readout **85** 1390
[217] Haefliger D, Marie R and Boisen A 2005 Self-actuated polymeric valve for autonomous sensing and mixing *13th Int. Conf. on Solid-State Sensors and Actuators and Microsystems, TRANSDUCERS '05 (Seoul, Korea)* p 1569
[218] Unterreithmeier Q P, Weig E M and Kotthaus J P 2009 Universal transduction scheme for nanomechanical systems based on dielectric forces *Nature* **458** 1001
[219] Schmid S, Senn P and Hierold C 2008 Electrostatically actuated nonconductive polymer microresonators in gaseous and aqueous environment *Sensors Actuators* A **145/146** 442
[220] Schmid S, Hierold C and Boisen A 2010 Modeling the Kelvin polarization force actuation of micro- and nanomechanical systems *J. Appl. Phys.* **107** 054510
[221] Mitra B and Gaitas A 2009 Thermally actuated tapping mode atomic force microscopy with polymer microcantilevers *Rev. Sci. Instrum.* **80** 023703
[222] Ilic B, Krylov S and Craighead H G 2010 Theoretical and experimental investigation of optically driven nanoelectromechanical oscillators *J. Appl. Phys.* **107** 13
[223] Ilic B, Czaplewski D, Zalalutdinov M, Craighead H G, Neuzil P, Campagnolo C and Batt C 2001 Single cell detection with micromechanical oscillators *J. Vac. Sci. Technol.* B **19** 2825
[224] Naik A K, Hanay M S, Hiebert W K, Feng X L and Roukes M L 2009 Towards single-molecule nanomechanical mass spectrometry *Nature Nanotechnol.* **4** 445
[225] Xu S and Mutharasan R 2009 Cantilever biosensors in drug discovery *Expert Opin. Drug Discov.* **4** 1237
[226] Senesac L and Thundat T G 2008 Nanosensors for trace explosive detection *Mater Today* **11** 28
[227] Blagoi G, Keller S, Johansson A, Boisen A and Dufva M 2008 Functionalization of SU-8 photoresist surfaces with IgG proteins *Appl. Surf. Sci.* **255** 2896
[228] Bietsch A, Zhang J Y, Hegner M, Lang H P and Gerber C 2004 Rapid functionalization of cantilever array sensors by inkjet printing *Nanotechnology* **15** 873
[229] http://www.cantion.com/CantiSpot.htm
[230] Weeks B L, Camarero J, Noy A, Miller A E, Stanker L and De Yoreo J J 2003 A microcantilever-based pathogen detector *Scanning* **25** 297
[231] Ramos D, Tamayo J, Mertens J, Calleja M, Villanueva L G and Zaballos A 2008 Detection of bacteria based on the thermomechanical noise of a nanomechanical resonator: origin of the response and detection limits *Nanotechnology* **19** 035503
[232] Ramos D, Tamayo J, Mertens J, Calleja M and Zaballos A 2006 Origin of the response of nanomechanical resonators to bacteria adsorption *J. Appl. Phys.* **100** 106105
[233] Gfeller K Y, Nugaeva N and Hegner M 2005 Micromechanical oscillators as rapid biosensor for the detection of active growth of *Escherichia coli Biosensors Bioelectron.* **21** 528
[234] Campbell G A and Mutharasan R 2005 Detection of pathogen *Escherichia coli* O157 : H7 using self-excited PZT-glass microcantilevers *Biosensors Bioelectron.* **21** 462
[235] Burg T P and Manalis S R 2003 Suspended microchannel resonators for biomolecular detection *Appl. Phys. Lett.* **83** 2698
[236] Burg T P, Godin M, Knudsen S M, Shen W, Carlson G, Foster J S, Babcock K and Manalis S R 2007 Weighing of

biomolecules, single cells and single nanoparticles in fluid *Nature* **446** 1066
[237] Zhang J, Lang H P, Huber F, Bietsch A, Grange W, Certa U, McKendry R, Guntgerodt H J, Hegner M and Gerber C 2006 Rapid and label-free nanomechanical detection of biomarker transcripts in human RNA *Nature Nanotechnol.* **1** 214
[238] Braun T, Ghatkesar M K, Backmann N, Grange W, Boulanger P, Letellier L, Lang H P, Bietsch A, Gerber C and Hegner M 2009 Quantitative time-resolved measurement of membrane protein–ligand interactions using microcantilever array sensors *Nature Nanotechnol.* **4** 179
[239] Pinnaduwage L A, Boiadjiev V, Hawk J E and Thundat T 2003 Sensitive detection of plastic explosives with self-assembled monolayer-coated microcantilevers *Appl. Phys. Lett.* **83** 1471
[240] Zuo G M, Li X X, Zhang Z X, Yang T T, Wang Y L, Cheng Z X and Feng S L 2007 Dual-SAM functionalization on integrated cantilevers for specific trace-explosive sensing and non-specific adsorption suppression *Nanotechnology* **18** 255501
[241] Datskos P G, Rajic S, Sepaniak M J, Lavrik N, Tipple C A, Senesac L R and Datskou I 2001 Chemical detection based on adsorption-induced and photoinduced stresses in microelectromechanical systems devices *J. Vac. Sci. Technol.* B **19** 1173
[242] Krause A R, Van Neste C, Senesac L, Thundat T and Finot E 2008 Trace explosive detection using photothermal deflection spectroscopy *J. Appl. Phys.* **103** 094906
[243] Yi D C, Greve A, Hales J H, Senesac L R, Davis Z J, Nicholson D M, Boisen A and Thundat T 2008 Detection of adsorbed explosive molecules using thermal response of suspended microfabricated bridges *Appl. Phys. Lett.* **93** 154102
[244] Senesac L R, Yi D, Greve A, Hales J H, Davis Z J, Nicholson D M, Boisen A and Thundat T 2009 Micro-differential thermal analysis detection of adsorbed explosive molecules using microfabricated bridges *Rev. Sci. Instrum.* **80** 035102
[245] Greve A, Olsen J, Privorotskaya N, Senesac L, Thundat T, King W P and Boisen A 2010 Micro-calorimetric sensor for vapor phase explosive detection with optimized heat profile *Microelectron. Eng.* **87** 696
[246] Petersen K E and Guarnieri C R 1979 Young's modulus measurements of thin films using micromechanics *J. Appl. Phys.* **50** 6761
[247] Taechung Y and Chang-Jin K 1999 Measurement of mechanical properties for MEMS materials *Meas. Sci. Technol.* **10** 706
[248] Srikar V and Spearing S 2003 A critical review of microscale mechanical testing methods used in the design of microelectromechanical systems *Exp. Mech.* **43** 238
[249] Li X, Ono T, Wang Y and Esashi M 2003 Ultrathin single-crystalline-silicon cantilever resonators: fabrication technology and significant specimen size effect on Young's modulus *Appl. Phys. Lett.* **83** 3081
[250] Nilsson S G, Borrise X and Montelius L 2004 Size effect on Young's modulus of thin chromium cantilevers *Appl. Phys. Lett.* **85** 3555
[251] Gavan K B, Westra H J R, van der Drift E W J M, Venstra W J and van der Zant H S J 2009 Size-dependent effective Young's modulus of silicon nitride cantilevers *Appl. Phys. Lett.* **94** 233108
[252] He J and Lilley C M 2008 Surface stress effect on bending resonance of nanowires with different boundary conditions *Appl. Phys. Lett.* **93** 263108
[253] Miller R E and Shenoy V B 2000 Size-dependent elastic properties of nanosized structural elements *Nanotechnology* **11** 139
[254] Sadeghian H, Yang C K, Goosen J F L, van der Drift E, Bossche A, French P J and van Keulen F 2009 Characterizing size-dependent effective elastic modulus of silicon nanocantilevers using electrostatic pull-in instability *Appl. Phys. Lett.* **94** 221903
[255] Nagy A, Strahl A, Neuhäuser H, Schrader S, Behrens I, Peiner E and Schlachetzki A 2004 Mechanical spectroscopy of thin layers of PPV polymer on Si substrates *Mater. Sci. Eng.* A **370** 311
[256] Jung N, Seo H, Lee D, Ryu C Y and Jeon S 2008 Nanomechanical thermal analysis of the glass transition of polystyrene using silicon cantilevers *Macromolecules* **41** 6873
[257] Jung N and Jeon S 2008 Nanomechanical thermal analysis with silicon cantilevers of the mechanical properties of poly(vinyl acetate) near the glass transition temperature *Macromolecules* **41** 9819
[258] Haramina T, Kirchheim R, Tibrewala A and Peiner E 2008 Mechanical spectroscopy of thin polystyrene films *Polymer* **49** 2115
[259] Pantazi A *et al* 2008 Probe-based ultrahigh-density storage technology *IBM J. Res. Dev.* **52** 493
[260] http://www.nanovlsi.caltech.edu/index.html